Long-term adaptation to hypoxia provides insight into mechanisms facilitating the switch of *Pseudomonas aeruginosa* to chronic lung infections.

Joanna Drabinska[1,2], Lucia O'Connor[1,2], Niamh Duggan[1,2], Ciarán J. Carey[1,2], Siobhán McClean[1,2]*

[1]School of Biomolecular and Biomedical Sciences, University College Dublin, Belfield, Dublin, Ireland.

[2]Conway Institute of Biomolecular and Biomedical Science, University College Dublin, Belfield, Dublin, Ireland.

*Corresponding author

Email: siobhan.mcclean@ucd.ie

Abstract

Opportunistic bacterial infections emerging from the environment are an increasing threat, especially for immunocompromised individuals such as people with cystic fibrosis (CF), driving morbidity, and mortality. *Pseudomonas aeruginosa* is a key pathogen from this group associated with chronic lung infections that has been extensively studied in this context, but the mechanism driving its adaptation towards chronic colonisation in the CF lung is not fully understood.

This work focuses on the adaptations of *P. aeruginosa* to long-term hypoxia, one of the important environmental pressures present in the CF lung, to investigate whether it drives the development of persistence in CF patients. We examined how an early CF isolate adapted to 6% oxygen over 28 days using an experimental evolution approach and showed that two distinct *P. aeruginosa* small colony variants (SCVs) emerged, one exclusively in hypoxia exposure cultures. Importantly, SCVs were more prevalent in hypoxia-adapted cultures than in normoxia-adapted cultures (98% vs <35%). Proteomic analysis revealed significant changes in the abundance of >200 proteins within 28 days, including proteins involved in antibiotic resistance, stress response, iron acquisition, biofilm formation and those previously associated with chronic infection. Importantly the observed changes in the proteome were distinct from changes reported after short-term exposure to hypoxia. Phenotypic characterisation of adapted cultures supported these findings, showing that hypoxia-adapted cultures developed higher resistance to 8 of 13 antibiotics tested; increased biofilm (1.8-4.1-fold ($p<0.0001$) and decreased pyocyanin production (2.6-fold, $p<0.0001$). All hypoxia-adapted cultures showed decreased siderophore production (2.9-3.6-fold, $p<0.02$). Two distinct patterns of adaptation to hypoxic conditions were observed, with the phenotypes of one culture being markedly different from the other two. Overall, we demonstrate that long-term hypoxia exposure contributes to multiple phenotype and proteome changes that are also observed in *P. aeruginosa* CF lung chronic infection, possibly opening the path to treatment of chronic infections.

Author Summary

Opportunistic antibiotic-resistant bacterial infections emerging from the natural environment are an increasing threat, particularly for immunocompromised individuals such as people with cystic fibrosis (CF). These infections increase disease severity, the number of deaths and healthcare costs. *Pseudomonas aeruginosa* is a major pathogen in this context, causing long-term infections, yet the mechanisms driving its adaptation towards chronic colonisation in the CF lung are not understood.

We investigated the adaptations of *P. aeruginosa* exposed to low oxygen conditions (an important environmental pressure in the CF lung), for 28 days, to examine whether it drives the process of persistence. We found that prolonged exposure to hypoxia induced changes in the pathogen's characteristics, which were distinct from those reported after short term exposure. We observed multiple adaptations in hypoxia adapted cultures, many of which were associated with important signalling networks linked to lifestyle shifts in most bacteria and several of them are also observed in isolates that had adapted to chronic infection. Similar adaptive responses in other opportunistic environmental pathogens suggest that this adaptation could be targeted to create universal therapeutic approaches preventing antibiotic overuse and improving patient outcomes.

Key words

Pseudomonas aeruginosa; hypoxia; adaptation; experimental evolution; chronic infection; cystic fibrosis

58 # Introduction

59 Antibiotic-resistant bacterial infections are a growing threat to society, were associated with nearly
60 five million deaths in 2019 (1), and are expected to cause more than 10 million deaths annually by
61 2050 (2). Opportunistic pathogens such as *Pseudomonas aeruginosa* play a crucial role in escalating
62 this crisis. While these bacteria typically do not cause infections in healthy people,
63 immunocompromised individuals and people with underlying conditions such as cystic fibrosis (CF)
64 and chronic obstructive pulmonary disease (COPD) or those on ventilator support are at great risk of
65 developing chronic *P. aeruginosa* lung infections (3,4). Moreover, opportunistic pathogens are
66 responsible for the majority of healthcare-associated infections, contributing to increasing morbidity,
67 mortality and costs (5).

68 *P. aeruginosa* is a Gram-negative opportunistic human pathogen, a leading cause of nosocomial
69 infections, constituting 11-26% of ventilator-associated pneumonia globally (6). Overall, it causes
70 more than 7% of all health-associated infections and is a major contributor to morbidity and mortality
71 among people with CF (7–9). It has many intrinsic and acquired mechanisms of antibiotic resistance
72 contributing to its spread and persistence (10), and prolonged antibiotic treatments necessary to
73 manage chronic infections contribute to the spread of antimicrobial resistance (11,12). Furthermore,
74 the World Health Organisation recognised *P. aeruginosa* as a high priority pathogen in 2024 while the
75 ECDC considers it a serious threat (13–16).

76 A key feature of *P. aeruginosa* is its exquisite metabolic flexibility and adaptability to harsh conditions,
77 allowing it to transition from the colonisation of the rhizosphere to colonising niches within human
78 or animal hosts (4), and establishing persistent infections (17). *P. aeruginosa* isolates from chronic
79 infections generally show different characteristics to those isolated from acute infections and chronic
80 infections are extremely difficult to eradicate. Its adaptability is driven by a complex regulatory

81 network involving transcriptional regulators, DNA modifications, non-coding RNAs, quorum sensing,
82 and a range of virulence factors (18–23). Despite this extensive research, the exact mechanism(s)
83 enabling *P. aeruginosa* to transition from acute to chronic infection remain unclear.

84 *P. aeruginosa*, a facultative anaerobe, thrives under low oxygen/anaerobic conditions using
85 alternative terminal electron acceptors and/or fermentation substrates. Previous studies showed that
86 *P. aeruginosa* preferentially colonizes hypoxic niches within mucus layers of the lung over more
87 oxygenated surfaces (24). *P. aeruginosa* responds to changes in oxygen levels via Anr, which regulates
88 the expression many of the genes shown to be altered in CF chronic infection (25,26). Studies on
89 another CF-associated pathogen, *Burkholderia cenocepacia* have shown that 40% of genes within a
90 low oxygen activated (Lxa) locus were upregulated in long-term infection isolates from CF patients
91 (27). We subsequently showed that deletion of single genes from the Lxa or the entire locus resulted
92 in changes in phenotypes crucial for the virulence of this bacterium including host cell attachment,
93 intracellular survival and stress responses (27,28). Given that hypoxia is an important environmental
94 pressure present in the lung, we wanted to evaluate the impact of long-term hypoxia exposure on *P.*
95 *aeruginosa.*

96 To examine the effect of long-term exposure to a low oxygen environment, we developed an
97 experimental evolution approach and demonstrated the significance of long-term exposure to low
98 oxygen conditions on the adaptation of *P. aeruginosa* to chronic lung infections. Our findings provide
99 new insights into the mechanisms that underlie the persistence and virulence of opportunistic
100 bacteria within the host.

101

102

103

Results

Design and Optimisation of Experimental Evolution

To investigate the impact of long-term exposure to low oxygen conditions on the adaptation of *P. aeruginosa*, we designed an experimental evolution approach (Fig 1A) exposing the *P. aeruginosa* early infection strain AMT 0023-30 (29,30) to either 6% oxygen or to normoxia (21%) for 28 days. This is a well-characterized and sequenced cystic fibrosis (CF) paediatric early infection strain that was selected from the international *P. aeruginosa* panel, for which a sequential chronic infection isolate is available (AMT 0023-31) (30–32). After considering ranges of oxygen bacteria are exposed to in soil and water, the range of hypoxic conditions in the CF lung and available literature on physiological tissue hypoxia (24,33,34), we chose 6% oxygen as it allowed us to observe the response to hypoxia, while not extensively stressing the cells and distinguish this response from changes associated with anoxia.

Daily culture transfer volumes were optimised by evaluating a range of volumes (1-10%) of overnight *P. aeruginosa* cultures transferred into fresh media and analysing their growth patterns (S1 Figure). A 5% volume transfer was chosen as optimal, as it allowed the transfer of the maximum number of bacterial cells without disrupting the growth pattern and resulted in a starting OD_{600} of ~0.1. Examination of growth patterns of the early infection strain revealed a significant difference in the generation times observed during hypoxic and normoxic conditions, with the strain growing 1.8-fold slower under hypoxia (g = 107 minutes) compared to normoxia (g = 60 minutes) (S2 Figure). Consequently, during the 28 day adaptation period, the cultures exposed to hypoxia underwent only 377 generations in contrast to 677 generations under normoxic conditions.

To facilitate further investigation, including phenotyping, proteome analysis, and whole genome sequencing (WGS), three independent flasks were inoculated and incubated under either 6% oxygen or normoxia (21% O_2), and samples were collected every day over 28 days, at time of culture transfer. The three 28 day independently adapted populations are referred to as N1, N2, and N3 for replicate normoxia-adapted control populations (NACs) and H1, H2, and H3 for the three replicate hypoxia-adapted cultures (HACs) (Table 1). All the phenotypic characterisation of the individual adapted populations (Both HACs and NACs) was performed under normoxic conditions, to ensure the observed changes are stable in the absence of continued hypoxia.

Table 1. List of strains and populations used in this study

Strain/Population Name		Description	Source
	E	Paediatric early infection cystic fibrosis strain AMT 0023-30	(29)
	L	Paediatric early infection cystic fibrosis strain AMT 0023-31	(29)
NACs	**N1**	28 day normoxia-adapted population, replicate 1	This study
	N2	28 day normoxia-adapted population, replicate 2	This study
	N3	28 day normoxia-adapted population, replicate 3	This study
HACs	**H1**	28 day hypoxia-adapted population, replicate 1	This study
	H2	28 day hypoxia-adapted population, replicate 2	This study
	H3	28 day hypoxia-adapted population, replicate 3	This study

Changes in colony morphology and pyocyanin production during adaptation

Changes in colony morphology often serve as key indicators of adaptation to the environment. Plating of daily samples from the adapting cultures showed the emergence of small colony variants (SCVs) both in NACs and HACs, however, the SCVs appeared earlier during hypoxia exposure (Fig 1B). SCVs first appeared on day 2 in the H3 population, and by day 3 in the H1 and H2 populations. The SCV abundance peaked at 98% on day 22, with 77% remaining on day 28 in H1. Similarly, the highest proportion of SCVs was reached on day 20 with 82% of the population and 80% on the last day of the experimental evolution experiment in flask H2. In contrast, in population H3 the SCV abundance was lower and more variable, reaching only 50% of the population by day 15, and falling to 1% on day 21.

147 The SCVs appeared much later in normoxic cultures, on days 6, 7 and 8 in flasks N1, N2 and N3
148 respectively and only reached a maximum of 25-33% of the population by day 14 (Fig 2A).

149 Two distinct SCV morphologies were observed (Fig 1C and D). The first type, termed SCV 1, was
150 observed both under normoxia and hypoxia and resembled the morphology most often described as
151 a rugose small colony variant characterised by small size, irregular edges and a heavily wrinkled, dry
152 surface (35). The second type, SCV 2, was slightly bigger than SCV 1 with a similar rough, dry surface;
153 however it was easily distinguished by a more regular edge and shape and importantly, it was
154 exclusive to HACs.

155 Throughout the 28 days of adaptation, we also observed dynamic changes in culture colour (Fig 2A),
156 suggesting changes in pigments, such as pyocyanin. Quantification of pyocyanin production at 28
157 days, despite almost no visible change of colour being observed on the day 28 of the experiment (Fig
158 2A), revealed that populations H1, H2 and one NAC, N1 produced comparable pyocyanin levels to the
159 late infection strain (AMT 0023-31) (Fig 2B and Fig 2C), suggesting that pyocyanin production is
160 independent of environmental oxygen levels.

161 Influence of hypoxia on the whole proteome

162 The proteomes of 28 day adapted cultures were analysed to elucidate the overall influence of long-
163 term hypoxia on *P. aeruginosa*. The individual flasks were treated as technical replicates, thus showing
164 the global changes across 3 independent populations. A total of 244 proteins showed significant
165 differences ($p \leq 0.05$) in abundance between 28 day HACs and 28 day NACs, of which 205 were altered
166 by 1.5-fold or more (Table 2, S3. Table). The majority of these proteins showed decreased abundance
167 following exposure to hypoxic conditions (n=148; 72.55%), while only 56 proteins (27.45%) showed
168 increased abundance (Table 2). A constructed heatmap showed divergence between the samples
169 from cultures adapted to the same condition (Fig 3A).

Table 2. Proteome comparison of 28 day hypoxia-adapted PA populations to normoxia-adapted populations.

Protein groups	Number of proteins*
Total number of identified proteins	1718
Proteins with significantly changed abundance (total)	244
Proteins with significantly changed abundance (by ≥1.5-fold)	205
Proteins unique to hypoxia	5
Proteins unique to normoxia (absent in hypoxia)	16
Proteins with a significantly increased abundance (by ≥1.5-fold) in hypoxia	56
Proteins with a significantly decreased abundance (by ≥1.5-fold) in hypoxia	149

*The proteins with significantly changed abundance were determined using mean LFQ intensities of three independent populations of normoxia and hypoxia-adapted cultures. A fold-change cutoff ≥1.5 was to compare hypoxic and normoxic conditions (T.test $p \leq 0.05$)

Functional enrichment

GO biological process functional enrichment analysis identified 35 enriched categories (S4 Table), including those associated with stimulus response, iron-sulphur cluster assembly, and amino acid metabolism. A separate analysis of proteins with increased or decreased abundance in HACs provided further insights into these important processes (Table 3, S2 Table). Overall, 38 GO biological processes were enriched in the increased abundance in hypoxia group (Fig 3B), while 37 processes were enriched in the decreased abundance group (Figure 3B; S2 Table). As expected, hypoxia led to upregulation of processes related to oxygen transport and nitrogen metabolism. Additionally, eight categories relating to nucleotide, nucleoside, ribonucleotide, and ribose phosphate processes were upregulated in hypoxia, together with those associated with gene expression, translation, peptide biosynthesis, and amide biosynthesis. Glutamate biosynthesis and glutamine family amino acid biosynthesis were the only two processes related to amino acid metabolism associated with increased abundance in HACs. In contrast, 18 categories related to amino acid metabolism, including those involving valine, tyrosine, phenylalanine, glutamate, and glutamine, were in the reduced abundance group, suggesting they may be downregulated. Sulphur and iron-sulphur cluster associated processes, chemotaxis, and motility were also associated with proteins that were reduced in abundance.

196 **Table 3. Comparison of GO term biological function enrichment of proteins increased in abundance,**

197 **decreased in abundance or both in the 28 day hypoxia adapted cultures**

Increased in abundance	Decreased in abundance
Amino acid metabolism *Glutamate biosynthesis*	Amino acid metabolism *Glutamate metabolism* *L-Phenylalanine metabolism* *Tyrosine catabolism* *Valine metabolism*
Oxygen transport	Iron-sulphur cluster assembley
Nucleotide metabolism *Nucleotide biosynthesis* *Ribonucleotide metabolism*	Response to stimulus *Locomotion* *Chemotaxis*
Protein metabolism	
Peptide biosynthesis	
Amide biosynthesis	
Gene expression	

Blue: functional enrichment of proteins increased in abundance in hypoxia adapted cultures; Orange: functional enrichment of proteins decreased in abundance in hypoxia adapted cultures.

A STRING local network cluster analysis confirmed that the processes associated with proteins that were increased in abundance included translation, protein synthesis, and nucleoside synthesis in hypoxia. It also revealed enrichment in proteins associated with glycolysis and pentose phosphate pathways, including those that were increased and decreased in abundance. Additionally, two mixed categories comprising the *P. aeruginosa* biofilm formation pathway appeared to be upregulated, based on changes in protein abundance. Beyond the downregulation of amino acid and chemotaxis-related pathways identified by GO term enrichment analysis, STRING analysis also highlighted reduced abundance of proteins associated with siderophore production, lipopolysaccharide biosynthesis, fatty acid degradation, quinone biosynthesis, and stress response pathways in hypoxia (S4 Table). KEGG pathway enrichment analysis further highlighted the upregulation of pyrimidine metabolism, ribosome biogenesis, and the alanine, aspartate, and glutamate pathways, alongside the downregulation of siderophore biosynthesis, propanoate metabolism, and amino acid metabolism under hypoxia (S4 Table).

221 **Proteins unique to hypoxia or normoxia**

222 Interestingly, 8.61 % of proteins that showed changes in abundance were either unique to HACs or
223 NACs, as they were present in one condition and were not detected in any of the 3 replicates in the
224 other group. Their consistent presence or absence across all three HACs suggests that their expression
225 is either switched on or off, and consequently, they play critical roles in adapting to low oxygen
226 environments. Only five proteins were unique to HACs (Table 4). These were associated with antibiotic
227 resistance, exopolysaccharide transport, glutamine and arginine metabolism and cell division. The
228 protein showing the highest abundance among these was PA4456, the ATP-binding component of an
229 ABC transporter. Although other ABC transporter components also showed changes in abundance,
230 they were less dramatic, with fold changes below 6.5-fold. Another protein unique to hypoxia, outer
231 membrane lipoprotein PelC is essential for Pel exopolysaccharide export (36). Glutamate
232 dehydrogenase GdhA, an enzyme in the glutamate biosynthesis pathway and arginine catabolism,
233 was also exclusively detected under hypoxic conditions. Finally, two hypothetical proteins were also
234 unique to HACs, PA3402, involved in transmembrane transport (37), and PA4278, identified as an *E.*
235 *coli* DedD homolog, a crucial component of the bacterial divisome (38).

236 Proteins that were absent in HACs, and thus potentially redundant in low oxygen conditions, are
237 involved in essential processes such as stress resistance, virulence, regulation (two-component
238 systems), polyamine catabolism, tryptophan biosynthesis, QS, bacterial competition, motility,
239 attachment, biofilm formation and antibiotic resistance (Table 4). Surprisingly, the NarL component
240 of the nitrate-responsive, Anr-regulated system crucial for anaerobic metabolism (39,40), was
241 undetectable in hypoxic conditions. Proteins important for *P. aeruginosa* virulence were also
242 undetectable in the HACs, including the HptA histidine phosphotransporter, a component of an
243 unorthodox/hybrid two-component system. NqrA NADH dehydrogenase is involved in bacterial
244 competition and protects *P. aeruginosa* against autotoxicity (41), while AsnB asparagine synthase and

245 YhfE glutamyl aminopeptidase are both involved in osmotic stress resistance and cell wall stress
246 response (42–45) and the Sbp substrate binding protein is associated with sulphate starvation
247 response and virulence (46,47), were all absent in HACs. Examples of proteins associated with biofilm
248 formation and/or motility that were absent in HACs, include the RidA deaminase (48,49), the PlaB
249 phospholipase B (50) and the PelC exopolysaccharide export associated protein.

250 **Table 4. Proteins unique to hypoxia-adapted or normoxia-adapted cultures grouped according to**
251 **function.**

Gene ID[a]	Protein Name	Protein Product Name	H/N[b]	NP[c]	MW[d]	SC[e]
		Stress response				
PA3459	**AsnB**	probable glutamine amidotransferase		8	66.03	17.50
PA3461	**YhfE**	conserved hypothetical protein		6	43.29	21.60
PA0283	**Sbp**	sulfate-binding protein precursor		4	36.43	20.20
		Biofilm/ exopolysaccharide production				
PA3062	**PelC**	PelC		6	18.68	58.10
PA0537	**PA0537**	conserved hypothetical protein		4	22.18	25.20
PA5234	**PA5234**	probable oxidoreductase		4	34.01	14.50
PA2927	**PlaB**	hypothetical protein		4	49.48	5.20
PA3123	**RidA**	RidA subfamily protein		4	34.40	13.52
		Amino acid metabolism				
PA4588	**GdhA**	glutamate dehydrogenase		4	48.85	13.5
PA3713	**SpdH**	spermidine dehydrogenase SpdH		9	68.86	19.5
PA0036	**TrpB**	tryptophan synthase beta chain		6	43.68	18.4
		Transport				
PA4456	**YrbF**	probable ATP-binding component of ABC transporter		5	29.62	26.00
PA3402	**PA3402**	hypothetical protein		5	36.21	21.10
		Other				
PA4278	**PA4278**	hypothetical protein		3	26.08	10.70
PA0991	**HptA**	Histidine phosphotransfer protein HptA		3	38.40	13.29
PA2999	**NqrA**	Na+-translocating NADH: ubiquinone oxidoreductase subunit Nrq1		2	48.08	6.10
PA3879	**NarL**	two-component response regulator NarL		4	24.26	30.10
PA2786	**PA2786**	hypothetical protein		4	17.54	33.50
PA3808	**IscX**	conserved hypothetical protein		4	7.80	62.10
		Function unknown				
PA2530	**PA2530**	hypothetical protein		7	48.96	22.00
PA5136	PA5136	hypothetical protein		3	54.32	6.90

252 [a]Gene ID – *Pseudomonas aeruginosa* PAO1 gene locus ID
253 [b]H/N – Blue: proteins unique to hypoxia-adapted cultures; Red: Proteins absent in hypoxia-adapted cultures
254 [c]NP - Unique peptides: The number of peptide sequences unique to a protein
255 [d]MW - Molecular weight as determined by Q-Exactive LC-MS using *P. aeruginosa* PAO1 reference
256 [e]SC - % sequence covered by matching peptides for the identified protein

257 Antibiotic resistance of adapted cultures

258 A change in the abundance of 48 proteins associated with antibiotic resistance was observed in HACs
259 (Table 5), with 25 showing increased abundance. Notably, type VI secretion system proteins, and TopA

260 topoisomerase, all previously associated with resistance to various classes of antibiotics, were
261 increased in abundance; however, in contrast, MexA and OprM efflux pump proteins, DNA turnover
262 proteins (e.g. elongation factor G, MutL) and cell envelope biosynthesis proteins showed decreased
263 abundance.

264 **Table 5. Examples of proteins altered by ≥ 1.5-fold in hypoxia-adapted cultures relative to normoxia-**
265 **adapted cultures.**

Gene ID[a]	Protein Name	Fold Change	Protein Product Name	Function[b]	UP[c]	MW[d]	SC[e]
PA3402	**PA3402**	U[f]	hypothetical protein	Antibiotic res	5	36.21	21.10
PA3062	**PelC**	U[f]	PelC	Biofilm	6	18.68	58.10
PA4456	**YrbF**	U[f]	probable ATP-binding component of ABC transporter	Antibiotic res	5	29.62	26.00
PA2664	**Fhp**	6.52	flavohemoprotein	Stress res	7	43.66	27.50
PA3163	**Cmk**	5.50	cytidylate kinase	Antibiotic res	3	24.64	21.80
PA5346	**SadB**	3.39	SadB	Biofilm, Motility	5	51.43	19.60
PA3559	**PA3559**	3.20	Probable nucleotide sugar dehydrogenase	Biofilm	3	51.80	10.60
PA0091	**VgrG1**	2.60	VgrG1	Antibiotic res	5	72.01	22.90
PA2900	**PA2900**	2.47	probable outer membrane protein precursor	Antibiotic res	5	29.85	30.90
PA4753	**YhbY**	2.46	conserved hypothetical protein	Antibiotic res	9	11.66	88.50
PA5549	**GlmS**	2.34	glucosamine-fructose-6-phosphate aminotransferase	Antibiotic res	30	66.29	49.60
PA0762	**AlgU**	2.19	Sigma factor AlgU	Biofilm, Motility	7	22.20	52.30
PA0083	**TssB1**	2.10	TssB1	Antibiotic res, Biofilm	13	18.79	73.80
PA0084	**TssC1**	2.00	TssC1	Antibiotic res, Biofilm	31	55.77	69.70
PA0141	**Ppk2**	1.97	GDP-polyphosphate phosphotransferase	Biofilm	20	40.79	72.80
PA4131	**PA4131**	1.90	probable iron-sulfur protein	Fe acq.	15	63.99	24.80
PA5117	**TypA**	1.88	regulatory protein TypA	Antibiotic res, Motility	22	66.93	35.70
PA0067	**PrlC**	1.85	oligopeptidase A	Antibiotic res, Motility	35	76.04	40.80
PA1673	**Mrh**	1.82	Microoxic hemerythrin	Biofilm	5	17.85	37.30
PA0998	**PqsC**	1.70	PqsC	Antibiotic res	16	38.24	55.50
PA3011	**TopA**	1.70	DNA topoisomerase I	Antibiotic res, Stress res, Biofilm	37	97.28	51.80
PA3617	**RecA**	1.60	RecA protein	Antibiotic res	12	36.88	36.40
PA4748	**TpiA**	1.59	triosephosphate isomerase	Antibiotic res	10	25.62	44.20
PA3810	**HscA**	1.57	Heat shock protein HscA	Fe acq.	13	66.45	22.60
PA0588	**yeaG**	-1.56	conserved hypothetical protein	Antibiotic res, Motility	55	73.72	67.70
PA4595	**ArtR**	-1.56	ATP-activated Repressor of T3SS regulator	Antibiotic res	39	61.32	61.40
PA5078	**OpgG**	-1.59	OpgG	Stress res, biofilm	14	59.48	34.90
PA2553	**PA2553**	-1.60	probable acyl-CoA thiolase	Antibiotic res	43	41.40	90.90
PA3529	**TsaA**	-1.66	alkylhydroperoxide reductase C	Stress res	28	21.82	84.00
PA4406	**LpxC**	-1.70	UDP-3-O-acyl-N-acetylglucosamine deacetylase	Antibiotic res	17	33.44	54.50
PA3723	**YqjM**	-1.72	probable FMN oxidoreductase	Antibiotic res, Stress res	24	40.32	80.40
PA0758	**PA0758**	-1.74	hypothetical protein	Stress res	10	30.88	47.50
PA2552	**AcdB**	-1.85	probable acyl-CoA dehydrogenase	Antibiotic res, Motility	14	40.91	46.40
PA2532	**Tpx**	-1.90	thiol peroxidase	Antibiotic res, Stress res, Biofilm	18	17.23	99.40
PA2071	**FusA2**	-1.96	elongation factor G	Antibiotic res	31	77.57	70.40
PA4946	**MutL**	-2.08	DNA mismatch repair protein MutL	Antibiotic res	12	69.75	25.60
PA4876	**OsmE**	-2.11	osmotically inducible lipoprotein OsmE	Stress res	7	12.52	41.20
PA1097	**FleQ**	-2.14	Transcriptional regulator FleQ	Biofilm, Motility	23	55.28	58.00
PA5285	**SutA**	-2.17	SutA	Biofilm	12	11.17	93.30
PA0427	**OprM**	-2.20	Major intrinsic multiple antibiotic resistance efflux outer membrane protein OprM precursor	Antibiotic res, Stress res	14	52.60	32.60
PA3017	**PA3017**	-2.32	Universal stress protein	Stress res	11	15.84	84.80
PA2015	**LiuA**	-2.38	putative isovaleryl-CoA dehydrogenase	Antibiotic res	20	42.21	55.80
PA2639	**NuoD**	-2.49	NADH dehydrogenase I chain C,D	Antibiotic res	27	68.32	50.30

PA1041	**PA1041**	-2.55	Probable outer membrane protein precursor	Biofilm	13	21.75	49.50
PA2009	**HmgA**	-2.55	homogentisate 1,2-dioxygenase	Stress res	17	47.84	50.50
PA3922	**PA3922**	-2.55	conserved hypothetical protein	Antibiotic res, Biofilm	17	51.23	54.30
PA0473	**PsfA**	-2.62	probable glutathione S-transferase	Fe acq.	6	28.33	22.90
PA1561	**Aer**	-2.65	Aerotaxis receptor Aer	Motility	18	57.18	45.70
PA5111	**GloA3**	-2.73	lactoylglutathione lyase	Antibiotic res	3	20.21	31.80
PA4290	**PA4290**	-2.92	probable chemotaxis transducer	Antibiotic res, Motility	16	58.40	37.20
PA4515	**PiuC**	-3.04	conserved hypothetical protein	Antibiotic res, Fe acq.	7	25.62	31.00
PA2867	**PA2867**	-3.07	Probable chemotaxis transducer	Motility	8	51.46	34.90
PA1753	**PA1753**	-3.10	conserved hypothetical protein	Antibiotic res, Stress res	4	18.37	33.30
PA4310	**PctB**	-3.13	Chemotactic transducer PctB	Motility	8	68.08	45.80
PA2008	**FahA**	-3.16	fumarylacetoacetase	Antibiotic res	15	46.34	41.20
PA2764	**PA2764**	-3.27	Hypothetical protein	Motility	7	24.52	33.30
PA0887	**AcsA**	-3.28	acetyl-coenzyme A synthetase	Antibiotic res	45	71.76	64.40
PA3795	**PA3795**	-3.50	probable oxidoreductase	Stress res	7	34.80	31.30
PA2920	**PA2920**	-3.57	probable chemotaxis transducer	Stress res, Motility	10	58.32	23.10
PA4221	**FptA**	-3.76	Fe(III)-pyochelin outer membrane receptor precursor	Fe acq.	25	79.99	42.20
PA4738	**YjbJ**	-4.09	conserved hypothetical protein	Stress res	5	7.61	75.40
PA2638	**NuoB**	-4.11	NADH dehydrogenase I chain B	Antibiotic res	9	25.43	36.40
PA0250	**PA0250**	-4.35	conserved hypothetical protein	Stress res	6	15.67	59.00
PA2652	**PA2652**	-4.67	Methyl-accepting chemotaxis protein	Motility	10	60.34	26.60
PA1092	**FliC**	-4.76	Flagellin type B	Bbiofilm, Motility	6	49.24	15.60
PA0425	**MexA**	-4.83	Resistance-Nodulation-Cell Division (RND) multidrug efflux membrane fusion protein MexA precursor	Antibiotic res	19	40.97	48.60
PA4223	**PchH**	-4.88	probable ATP-binding component of ABC transporter	Antibiotic res, Motility	9	61.34	20.70
PA0744	**PA0744**	-4.89	Probable enoyl-CoA hydratase/isomerase	Mot	14	40.59	38.70
PA3938	**TauA**	-5.11	probable periplasmic taurine-binding protein precursor	Antibiotic res, Stress res	9	35.86	50.10
PA3812	**IscA**	-5.34	probable iron-binding protein IscA	Antibiotic res, Fe acq.	4	11.57	51.40
PA3819	**YcfJ**	-5.67	conserved hypothetical protein	Antibiotic res, Stress res	9	18.97	63.20
PA2363	**HsiJ3**	-5.94	HsiJ3	Antibiotic res	5	47.78	19.20
PA4225	**PchF**	-5.98	pyochelin synthetase	Fe acq.	67	197.08	38.50
PA2788	**PA2788**	-6.13	Probable chemotaxis transducer	Motility	14	56.39	36.90
PA4226	**PchE**	-6.46	dihydroaeruginoic acid synthetase	Fe acq.	47	156.42	34.10
PA4224	**PchG**	-7.13	pyochelin biosynthetic protein PchG	Fe acq.	12	37.70	35.50
PA1065	**PA1065**	-7.68	conserved hypothetical protein	Antibiotic res	3	17.99	24.20
PA3441	**SsuF**	-7.71	probable molybdopterin-binding protein	Stress res	3	7.59	47.90
PA4230	**PchB**	-7.77	salicylate biosynthesis protein PchB	Antibiotic res, Fe acq.	12	11.43	62.40
PA2640	**NuoE**	-8.00	NADH dehydrogenase I chain E	Antibiotic res, Mot	6	18.09	60.20
PA2717	**Cpo**	-8.42	chloroperoxidase precursor	Stress res, Biofilm	9	30.44	59.10
PA2033	**ViuB**	-10.88	hypothetical protein	Fe acq.	6	33.65	28.50
PA5131	**Pgm**	-12.57	phosphoglycerate mutase	Antibiotic res	7	55.60	17.70
PA4825	**MgtA**	-17.09	Mg(2+) transport ATPase, P-type 2	Stress res, Fe acq.	41	100.05	32.80
PA4227	**PchR**	-20.62	transcriptional regulator PchR	Fe acq.	3	32.34	14.90
PA0283	**Sbp**	U[f]	sulfate-binding protein precursor	Stress res	4	36.43	20.20
PA0537	**PA0537**	U[f]	Conserved hypothetical protein	Biofilm	4	22.18	25.20
PA2786	**PA2786**	U[f]	hypothetical protein	Antibiotic res	4	17.54	33.50
PA2927	**PlaB**	U[f]	Hypothetical protein	Biofilm	4	49.48	5.20
PA3123	**RidA**	U[f]	RidA subfamily protein	Biofilm, Motility	4	13.52	34.40
PA3459	**AsnB**	U[f]	probable glutamine amidotransferase	Stress res	8	66.03	17.50
PA3461	**YhfE**	U[f]	conserved hypothetical protein	Stress res	6	43.29	21.60
PA3808	**IscX**	U[f]	conserved hypothetical protein	Fe acq.	4	7.80	62.10
			Increased in abundance (fold)		1.5-2	2-5	≥5
			Decreased in abundance (fold)		1.5-2	2-5	≥5

Blue shading represents proteins increased in abundance or unique to hypoxia. Dark blue: ≥5-fold increase in abundance; medium blue: 2-5-fold increase in abundance, light blue: 1.5-2-fold increase in abundance. Orange shading represents proteins decreased in abundance in hypoxia or absent in hypoxia. Dark orange: ≥5-fold decrease in abundance; medium orange: 2-5-fold decrease of abundance; light orange: 1.5-2-fold decrease in abundance.

[a]Gene ID – *Pseudomonas aeruginosa* PAO1 gene locus ID.

[b]Relevant protein function. Antibiotic res: antibiotic resistance; Stress res: stress resistance; biofilm: Biofilm formation and/or exopolysaccharide production; Fe acq.: iron acquisition and/or homeostasis; Motility: motility.

[c]UP - Unique peptides: The number of peptide sequences unique to a protein

[d]MW - Molecular weight as determined by Q-Exactive LC-MS using *P. aeruginosa* PAO1 reference (kDa)

[e]SC - % sequence covered by matching peptides for the identified protein

276 [f]U – Proteins unique to hypoxia or absent in hypoxia

277 To confirm whether the alterations of proteins associated with antibiotic resistance affect the
278 phenotype of each of the individually adapted cultures, antibiotic susceptibility was examined.
279 Changes in sensitivity to a wide range of antibiotic classes were observed in both populations (Fig 4).
280 However, both H1 and H2 populations clearly showed more increases in antibiotic resistance than any
281 other cultures, correlating with the changes in protein abundance. Increased resistance to
282 fluoroquinolones, macrolides, cephalosporins, carbapenems and penicillins was observed in both H1
283 and H2 cultures, together with decreased resistance to aztreonam. Interestingly, H3 culture only
284 showed an increased resistance to aztreonam with no change in susceptibility to any other antibiotic
285 tested. All strains were resistant to tetracycline.

286 Hypoxia-adapted cultures show changes in stress response

287 Many proteins related to stress responses showed changes in abundance in response to long-term
288 exposure to hypoxia (Table 4), including universal stress proteins (PA3017, PA1753); osmotic stress
289 response associated proteins (OpgG, OsmE, PA2920, PA4738, PA3461, AsnB); oxidative stress
290 response associated proteins (Ftp, TsaA, PA3723, Tpx, PA0250, TauA, OprM, MexA, TopA, Hmg, Cpo);
291 heat-shock stress response associated proteins (TopA, PA0758), sulphate starvation (SsuF, Sbp); cell
292 wall stress/envelope stress response proteins (PA3819, PA3795) and cadmium stress response (MgtA)
293 (Table 5). To examine the impact of these alterations on phenotype of each of the individual
294 populations, droplet stress plates were prepared to test a range of stresses described as hallmarks of
295 the CF lung environment. No clear pattern resistance to high temperature, osmotic or acidic stress
296 between the HACs and NACs was observed (Fig 4). Interestingly, increased resistance to oxidative
297 stress was observed in both H1 and H2 cultures and in the N3 culture, which were also the only
298 populations where SCVs had been detected on day 28, and where increased biofilm production and
299 exopolysaccharide production were observed (Fig 4).

300 **Hypoxia-adapted cultures show increased biofilm formation and**

301 **exopolysaccharide production**

302 Typically anaerobic conditions promote biofilm formation, with greater numbers of live bacteria,
303 increased thickness, and more compact structures (51). Changes in the abundance of 20 proteins
304 associated with biofilm and/or exopolysaccharide production were observed (Table 5). Nine showed
305 increased abundance or were unique to hypoxia, including the PelC exopolysaccharide export protein,
306 as already mentioned. Others included proteins involved in surface attachment (SadB),
307 exopolysaccharide production (PA3559, AlgU), and type VI secretion system (TssB1, TssC1). Proteins
308 that showed decreased abundance are involved in the switch from a planktonic to a biofilm lifestyle
309 (RidA), biofilm formation and structure, and cell attachment (PlaB, PA1041, SutA, FleQ, OpgG),
310 alginate production (Cpo), and flagellin (FliC).

311 To confirm the impact of these proteome changes on biofilm and exopolysaccharide production,
312 these phenotypes were examined in each individual adapted culture (Fig 5A, Fig 5B). Only H1 and H3
313 populations showed a significantly increased biofilm formation as compared to the early infection
314 patient isolate (6.1- and 4.3-fold increases respectively) after 24 h, although significant increases in
315 biofilm production were also observed in the late strain (1.6-fold), H1 (3.9-fold) and H2 (1.4-fold) over
316 the early strain at 48 h, and this trend persisted at 72h (Fig 5A). The increased biofilm production of
317 the H3 population was transient and reverted to AMT 0023-30 strain levels by 48 hours. Congo Red
318 staining revealed darker colonies for H1 and H2 populations which were more wrinkly than in the
319 other strains indicating a higher production of exopolysaccharides (Fig 5B). Interestingly, a similar
320 phenotype was observed in culture N3, again suggesting that this phenotype is not dependent on
321 oxygen exposure.

322

323 ## Adaptation to hypoxia affected iron acquisition and homeostasis

324 Proteomic analysis showed changes in the abundance of 14 proteins related to iron homeostasis and
325 acquisition pathways (Table 5). More than half of the proteins in the pyochelin biosynthesis pathway
326 were decreased in abundance by 6-fold or more (PchB, PchE, PchF, PchG) (Fig 5C), and the master
327 regulator of pyochelin production, PchR, was decreased in abundance by over 20-fold. Additionally,
328 the abundance of several iron transport proteins was decreased, including FptA (iron-bound
329 pyochelin receptor), ViuB (siderophore uptake protein), PiuC (Fe(II)-dependent dioxygenase), MgtA
330 (involved in citrate-bound iron transport into the cell), and PsfA (a stress protein involved in iron
331 acquisition). Moreover, the abundance of proteins involved in iron-sulphur cluster biosynthesis was
332 also affected by hypoxia with HscA increased in abundance nearly 1.6-fold, IscA decreased in
333 abundance over 5.3-fold and IscX undetectable in HACs.

334 Differences in iron acquisition and consequently siderophore levels of all individual populations were
335 examined and results were consistent with the overall proteome analysis, showing a clear decrease
336 in siderophore production in all of the HACs by 2.8- to- 3.6-fold ($p<0.05$), but no significant changes
337 in the NACs (Fig 5D). Moreover, a similar change was observed between the early infection isolate
338 and late infection isolate, with a 4-fold decrease in siderophores ($p<0.01$).

339 ## Adaptation to hypoxia induces changes in motility

340 Over 16 proteins associated with motility showed decreased abundance in the HACs, while only three
341 (flagellar reversal regulator SadB, TypA GTPase and the PrlC oligopeptidase), were increased in
342 abundance (Table 5). The proteins showing decreased abundance included those directly associated
343 with motility (FliC, FleQ, PA0588, PchH, NuoE) and a large group of chemotaxis associated proteins
344 (PA4290, PA2867, PctB, PA2920, PA2652, PA2764, AcdB, PA0744, PA2788) and receptor protein Aer,

345 suggesting that motility was downregulated in HACs. Notably, many of these proteins are also
346 associated with biofilm formation and antibiotic resistance.

347 To elucidate the effect of hypoxia on motility further, the motility of the individual cultures was
348 assessed. The late patient isolate showed a 2-fold reduction in swarming ($p<0.05$) (Fig 6B) and a
349 moderate reduction in twitching motility (1.3-fold; $p<0.01$) (Fig 6C), while H1 and H2 showed an
350 increased ability to swim (1.5 and 1.2-fold, $p<0.05$) compared to the early infection strain (Fig 6A). All
351 forms of motility were decreased in culture H3 by over 2.4-fold ($p<0.01$) (Fig 6A, 6B, 6C). A similar
352 pattern was observed in culture N3, with a 1.6-fold decrease in swimming motility ($p<0.05$) and a 1.9-
353 fold decrease in twitching motility ($p<0.01$) (Fig 6A, 6C). The pattern of swarming motility was clearly
354 different between NACs and HACs. N1 and N2 populations showed a classic swarming pattern with
355 clearly distinguishable dendrites despite showing no changes in diameter (Fig 6B). N3 showed a
356 different pattern, forming colonies with smooth edges. The H1 and H2 colonies on swarm plates were
357 clearly distinguishable from the N1 and N2 counterparts, with no clear dendrites being formed (Fig
358 6).

359 Effects of hypoxia-adaptation on *in vivo* virulence

360 The proteome and phenotype characterisation of HACs showed that adaptation to hypoxia altered
361 the abundance of proteins involved in virulence, and the appearances of many virulence associated
362 phenotypes, including SCV formation, stress and antibiotic resistance, and motility. Unexpectedly
363 however, no differences in virulence were observed *in vivo* in *Galleria mellonella* between the early
364 infection isolate and the HACs (Fig. 6D).

365

366

Discussion

Summary

Understanding the complex network of pathway interactions and the evolutionary pressures *P. aeruginosa* undergoes in different environments is the key to understanding its biology and the mechanisms behind chronic infection, facilitating the development of effective therapeutics. Hypoxic niches are abundant in the CF lung due to increased mucus thickness, obstructive mucus plugging and increased oxygen consumption by epithelial and immune cells (24,52,53). Studies have shown that microaerobic respiration is the predominant mode of *P. aeruginosa* growth in the CF lung (54,55), with two transcription factors, Anr and Dnr, tightly regulating the response to changes in oxygen tension (56,57), and giving *P. aeruginosa* the ability to respond to changes in oxygen concentration along a continuum (25).

While the impact of short-term hypoxia on *P. aeruginosa* has been previously studied (a few hours, until reaching OD_{600} = 1.0), the impact of hypoxia stress has not been examined over extended periods. We demonstrate that prolonged low oxygen conditions alone can induce stable proteomic and phenotypic changes which are typically associated with chronic infection, and thus potentially facilitate the transition from acute to chronic infection.

Diverse patterns of adaptation to long-term hypoxia

We have observed two distinct patterns of adaptation of *P. aeruginosa* to hypoxic conditions, consistent with existing literature which demonstrates evolution of different phenotypic and genetic characteristics with bacterial populations isolated from the same lung niche, or different parts of the biofilm, enabling bacterial competitiveness (22,58–62). Flynn et. al (2006), using a similar experimental evolution approach as we used in this work, albeit over 90 days, compared three biofilm

389 cultures and three planktonic cultures of *P. aeruginosa* PA14 and determined that different
390 phenotypes appeared at different intervals with different abilities to persist not only between
391 replicate cultures, but even between colonies isolated from the same population (59). Furthermore,
392 the various colony morphologies observed in this study correlated with temporal variations in c-di-
393 GMP levels (59), which aligns with the changes in the abundance of proteins associated with the
394 response to c-di-GMP in HACs.

395 Two of the HACs in our study (H1 and H2) showed consistent alterations across multiple phenotypes,
396 while the third population displayed only slight alterations relative to the early strain and were
397 effectively comparable to the NACs (Fig. 7A). This was confirmed by a phylogenetic tree that we
398 generated based on our sequencing data (data unpublished), which showed that H1 and H2 are
399 closely related to each other, but distant from all other populations, and the third HAC was most
400 closely related to the N3 population (Fig 7B). Previous investigation of the short term hypoxia
401 response (over 24 hours) revealed that the proteome changes were strain-specific (63), suggesting
402 that different adaptation patterns can occur as the population diversifies over the longer term. A
403 further, deeper analysis of the WGS data will allow us to elucidate the genetic background of the
404 observed differences.

405 Adaptation of *Pseudomonas aeruginosa* to long-term hypoxia is consistent 406 with changes observed during chronic infection

407 Interestingly, the adaptation of *P. aeruginosa* to long-term hypoxia mirrors the phenotypic and
408 molecular changes that have been reported for *P. aeruginosa* late infection isolates as a result of
409 adaptation to chronic infection (8,18,20,23,35,62,64). These include increased SCV prevalence,
410 increased biofilm and exopolysaccharide production, increased antibiotic resistance and decreased

411 siderophore production. The stability of these changes was evident, as all the phenotypes were tested
412 in normoxic conditions.

413 The first phenotypic change observed during the experimental adaptation of *P. aeruginosa* to long-
414 term hypoxia was the emergence of two distinct SCV types. They were more prevalent in the HACs,
415 and one of the morphotypes was exclusive to hypoxia. Surprisingly, the abundance of c-di-GMP
416 signalling pathways proteins, Wsp and YfiBNR, typically associated with SCVs (35,65), were unchanged
417 in the HACs, suggesting an alternative mode of regulation. SCVs are strongly associated with
418 pathogenicity and persistence among several bacterial pathogens, (66–68) and are prevalent among
419 chronic *P. aeruginosa* isolates (66,67,69). Specifically, SCVs of *P. aeruginosa* correlate with increased
420 exopolysaccharide and biofilm production, antimicrobial resistance, stress resistance and host
421 immune responses (35,69). Their emergence has been linked to redox imbalances which can be
422 caused by low oxygen conditions (70), although other environmental stressors or co-colonisation with
423 other species also contribute to their increased prevalence (66,69,71). This confirms directly, for the
424 first time, that prolonged hypoxia exposure is associated with increased SCV occurrence in *P.*
425 *aeruginosa* populations. Although SCVs temporarily occurred under normoxic conditions, they were
426 not selected as a beneficial trait in the longer term. Identification of the factors that contribute to SCV
427 emergence will be crucial due to the challenges they pose in clinical settings (66) and recognising the
428 environmental factors that select this phenotype may help us limit their occurrence.

429 Chronic infection *P. aeruginosa* CF isolates typically exhibit increased biofilm and exopolysaccharide
430 production, and reduced motility (18,62,72–74), with biofilm formation relying on hypoxia responses
431 due to the presence of steep oxygen gradients (26,75,76). Moreover, the awareness of the role of
432 biofilms in antibiotic treatment efficiency is being acknowledged increasingly (77,78).

433 The two HACs that showed a high SCV prevalence (H1, H2) also showed increased resistance to a
434 broad spectrum of antimicrobials together with increased biofilm and exopolysaccharide production.

435 Surprisingly, no trends in motility relating to hypoxia exposure or biofilm formation were observed,
436 although some changes in patterns of swarming colonies were noted.

437 Proteins associated with biofilm formation, exopolysaccharide production and motility were changed
438 in abundance, including an increase of abundance of SadB, which is required for irreversible cell
439 attachment, exopolysaccharide production and is associated with decreased swarming motility
440 (79,80), and the alternative sigma factor AlgU (σ22), which is one of the key factors leading to the
441 development of chronic *P. aeruginosa* infection in the CF lung and regulates the mucoid phenotype,
442 and contributing to stress and antibiotic resistance (81–83). A interesting cascade of regulation is
443 observed, as both SadB and AlgU act through the c-di-GMP and Gac/Rsm signalling pathways (84–
444 86). Further AlgU inhibits the FleQ master regulator of flagellar motility and exopolysaccharide
445 secretion, indirectly decreasing the abundance of the FliC flagellin type B (87). Noteworthy, another
446 modulator of the virulence, biofilm and antibiotic resistance of many Gram-negative bacteria, the
447 TypA GTPase (88,89), was also increased in abundance in HACs.

448 Antibiotic resistance is a major hallmark of *P. aeruginosa* infections in CF (90), and short-term hypoxic
449 and anaerobic conditions have been previously shown to increase *P. aeruginosa* antibiotic resistance
450 (91–93). We demonstrate that long-term exposure to hypoxia can induce stable changes in resistance
451 to antibiotics, which didn't revert following subsequent culture in normoxic conditions during
452 phenotyping or other investigations. Additionally, a wider range proteins associated with antibiotic
453 resistance were altered in abundance, including an increase in abundance of secretion systems
454 proteins and ABC transporter systems, outer membrane proteins, the TopA topoisomerase,
455 peptidoglycan/LPS biosynthesis proteins and quinolone signalling proteins. Disc diffusion assays
456 confirmed that two of the HACs showed increased resistance to a wide range of antibiotics from
457 different classes, further supporting the evidence of the extent of the influence of hypoxia pre-
458 adaptation on drug resistance and the wide range of diverse mechanisms affected.

459 Bacteria that colonise the CF lung undergo constant stress, including increased osmotic, acid and
460 oxidative stress (53,94,95). An increased resistance to oxidative stress and increased antibiotic
461 resistance was observed in two HACs, H1 and H2, which aligns with the available literature data
462 showing that preexposure to oxidative stress increases the resistance to many antibiotics (96–98).
463 Considering responses to different stress conditions involve overlapping systems (99), prolonged
464 hypoxia adaptation is likely to drive the organism's stress resistance in general. Understanding the
465 specific dynamics of this co-dependency may guide therapy choices in the future (Dawan & Ahn,
466 2022).

467 The airways of people with CF are reported to show an increased abundance of available iron
468 (101,102). *P. aeruginosa* expresses many iron acquisition systems including siderophore production,
469 haem acquisition systems and complexes importing iron-bound citrate or catechol (Schalk & Perraud,
470 2023). Importantly, a strong positive correlation between increased sputum iron and chronic *P.*
471 *aeruginosa* infections has been shown (104). HACs showed a decrease in the abundance of proteins
472 involved in pyochelin production (Pch cluster proteins), iron/siderophore uptake proteins/receptors
473 (FptA and ViuB), and citrate-bound iron transporter MgtA and PsfA, which alters iron uptake under
474 stress which correlate with the reports of low activity of pyochelin in CF sputum (105). The highly
475 conserved iron-sulphur cluster group, which includes the IscA and IscX (both of which were decreased
476 in abundance in HACs) is associated with iron storage and homeostasis, but also respiration, DNA and
477 RNA repair contributing to adaptation to various environments (106–108). Furthermore, iron uptake
478 and homeostasis are regulated by the c-di-GMP through the Gac/Rsm cascade (109), in line with other
479 alterations observed and underlines the role of hypoxia leading to changes in iron acquisition on
480 chronic infection development, which led to recognising them as therapy targets for *P. aeruginosa*
481 treatment (102,110).

482 It has been shown that exposure to hypoxia attenuated the virulence of isolates from acute, but not
483 chronic infections (111) and decreased their interactions with host cells, demonstrating the
484 importance of this environmental pressure. Moreover, despite the lower bacterial concentrations *in*
485 *vivo* in hypoxia, the mortality of mice was accelerated (112,113). Previous reports demonstrated that
486 decreased pyocyanin production is a characteristic of chronic infection (114). However, no changes in
487 the abundance of proteins associated with this phenotype were detected in HACs, and its production
488 was decreased in both HACs and NACs, suggesting that even though hypoxia may contribute to
489 reduced pyocyanin production, it is not dependent on low oxygen conditions. Additionally, we haven't
490 observed any changes in the *Galleria mellonella* infection model related to hypoxia exposure.

491 A recent study defined 224 genes of *P. aeruginosa* as pathoadaptive, and determined that the
492 expression of certain genes was associated with the host preference towards people with CF (116).
493 Nine proteins increased in abundance in HACs were encoded by pathoadaptive genes identified by
494 Weimann et al., including AlgU, FleQ, NarL, FptA, MexA, MutL, OprM, YrbF (previously discussed) and
495 additionally the RmlB rhamnose/lipopolysaccharide biosynthetic protein (117,118). Moreover, our
496 proteomics analysis showed changes in the abundance of 21 proteins encoded by genes whose
497 expression was positively associated with CF host preference and 38 that were associated with non-
498 CF infections (116), suggesting long-term hypoxia may play a role in *P. aeruginosa* infection both in CF
499 and non-CF cohorts. Although many of the phenotypes that were altered by extended culturing in
500 hypoxia can contribute to the pathogenicity of *P. aeruginosa*, the virulence of the HADs was
501 unchanged in the *G. mellonela* infection model. However, this is an acute infection model, and
502 consequently is not an optimal model to assess the impact of long-term hypoxia adaptation on
503 chronic infection.

504

505 **Differences between long-term adaptation and short-term response to**
506 **hypoxia**

507 The influence of various environmental pressures on the metabolism of pathogenic bacteria is
508 typically investigated by exposing bacteria to that factor for 24 h or less, which captures early
509 responses, but it does not evaluate the prolonged environmental pressures experienced during
510 infection. No studies on the effects of long-term exposure to hypoxia have been investigated in *P.*
511 *aeruginosa*.

512 Our findings highlight that the bacterial strategies employed to overcome short-term and long-term
513 stress exposure are quite distinct. Short-term adaptation facilitates quick, immediate responses
514 including the stringent response and/or metabolic adjustments, whereas prolonged exposure to
515 specific conditions is more likely to foster adaptation through the acquisition and accumulation of
516 genetic changes (119–122). Specific examples include the osmotic stress response of *Pseudomonas*
517 *putida,* which initially involved upregulation of osmoprotectant production, while long-term exposure
518 led to adjustments in the outer membrane's composition to reduce permeability (99). Furthermore,
519 *Helicobacter pylori* responded to acidic stress by rapidly expressing urease to neutralise the acid, but
520 over time altered its membrane structure and proton-pumping systems (123).

521 To date, only one study has specifically investigated the global proteome changes in response to short-
522 term hypoxia (63). In contrast, to the that study, which examined the *P. aeruginosa* PAO1 reference
523 strain and two adult cystic fibrosis strains (PASS2, PASS3), we used an early-infection paediatric isolate
524 (AMT 0023-30) with no prior lung adaptation, providing a unique perspective (29,30,32). Only three
525 proteins among the 101 proteins that changed in abundance both after long-term and short-term
526 hypoxia exposure were consistently altered across all four strains examined in both studies,
527 highlighting key proteins for hypoxia adaptation: the Mhr microaerophilic hemerythrin and the

528 PA0141 GDP-polyphosphate phosphotransferase were increased in abundance in hypoxia, while the
529 MaiA maleylacetoacetate isomerase decreased in abundance. Their role(s) in the pathogenicity of *P.*
530 *aeruginosa* suggests they may be promising candidates for further studies in relation to chronic
531 infection and its treatment (124–127). The abundance of 107 proteins was altered only in long-term
532 hypoxia cultures, but not after short-term exposure. Of the 31 proteins uniquely increased in
533 abundance during long-term adaptation, notable examples previously connected to chronic infection
534 adaptation and/or virulence include the AlgU sigma factor, T6SS-associated proteins, transporters,
535 and LPS associated proteins. Contrary to short-term hypoxia exposure which led to changes in the
536 abundance of cytochromes and denitrification pathways, no changes in the abundance of these
537 groups were detected in the long-term HACs. Additionally, no increases in the abundance of proteins
538 involved in oxidative stress resistance were observed, unlike the reported short-term hypoxia
539 response (63). This suggests that while oxidative stress responses are crucial for initial response to
540 low oxygen conditions, they are unlikely to play a significant role in the adaptation to prolonged
541 hypoxia.

542 Hypoxia-induced redox imbalance changes c-di-GMP levels

543 Hypoxia causes a redox imbalance in the bacterial cell which needs to be mitigated for the
544 maintenance of function and viability, and this process is regulated by c-di-GMP signalling. Previous
545 studies reported the role of c-di-GMP in regulating low oxygen response and stress resistance in *P.*
546 *aeruginosa* and highlight its function in the metabolic switch in response to environmental stimuli
547 including the switch from a planktonic to a biofilm lifestyle (85,128,129)**.** Moreover, the changes in c-
548 di-GMP levels were associated with diversification of populations and variability in phenotypes
549 expressed after adaptation to one condition (59). As we identified several proteins associated with
550 the GacAS system, it is tempting to speculate that hypoxia modulates the second messenger c-di-
551 GMP and consequently alters multiple c-di-GMP-regulated phenotypes, including the increased

552 biofilm formation and exopolysaccharide production, altered motility, and increased antibiotic
553 resistance we observe. For example, FleQ is a c-di-GMP receptor regulating biofilm formation,
554 exopolysaccharide production, and type VI secretion system expression (130–132). Considering the
555 above, we speculate that hypoxia adaptation modulates the swich from acute to chronic infection
556 through the c-di-GMP second messenger.

557 Common adaptation mechanisms of opportunistic pathogens to hypoxia

558 Several oxygen-sensing mechanisms, homologous genes in hypoxia regulons and several phenotypes
559 altered in chronic infection are shared across other opportunistic bacteria causing pulmonary
560 infections (Carey et al., *under review).* This suggests that adaptation to prolonged hypoxia could be a
561 shared mechanism between many low oxygen and/or microaerophilic habitats and are not limited to
562 human infections. These environments are increasingly abundant in water and soil, where
563 opportunistic bacteria reservoirs exist and play significant roles in shaping their physiology, with
564 increasingly contributing to their increased prevalence (133–137). As many opportunistic bacterial
565 pathogens causing CF infections reside in these niches, common adaptations are not unexpected.

566 Proteome analysis of HACs showed a decrease in abundance of ten proteins encoded on the Anr
567 regulon (56) that are involved in energy and amino acid metabolism (Qor, Hpd, GapN, PepN), or
568 associated with pathogenesis (LpxC – lipopolysaccharide production; ArtR – T3SS activity regulation;
569 Aer, PA2867 – chemotaxis/motility). Meanwhile, two proteins involved in biofilm production, Ppk2
570 and Mrh were increased in abundance after long-term hypoxia adaptation. Anr was reported to show
571 high activity in chronic *P. aeruginosa* infection isolates (25,26). It is noteworthy that its regulon shares
572 homologous genes with the DosR regulon of *Mycobacterium abscessus* and Lxa locus of *Burkholderia*
573 *cenocepacia* (Carey et al., *under review*), highlighting that aspects of the hypoxia response may be
574 shared across several opportunistic CF lung infections more generally. Targeting shared mechanisms

575 of adaptation to chronic infection could present a new opportunity for the treatment of multiple
576 pathogens simultaneously.

577 Impact

578 Recognizing the adaptive patterns of microorganisms is critical to devising targeted treatment
579 approaches. Crucially, this study demonstrates that alterations in phenotype after long-term exposure
580 to hypoxic conditions shows several similarities with those observed during adaptation to chronic
581 infection. Thus, further development of our understanding of the specific mechanisms by which *P.*
582 *aeruginosa* adapts to hypoxia in chronic infection and the interplay with other factors present in the
583 lung environment will potentially enable us to prevent or treat the switch from acute to chronic
584 infection. This could inevitably limit antibiotic use, severity of the disease and ultimately, decrease
585 the socioeconomic impact of infections caused by *P. aeruginosa*. Furthermore, the first drug to alter
586 the human response to hypoxia was recently approved for use by the FDA (138), thus it is tempting
587 to speculate that the response of bacteria to low oxygen pressures could be targeted to prevent a
588 switch from acute to chronic infection.

589 To summarise, the changes in proteome and phenotypes (increased biofilm formation, increased
590 antibiotic resistance, decreased siderophore production, increased SCV prevalence) further deepens
591 the knowledge on how hypoxia leads to adaptation of *P. aeruginosa*, shedding light on how prolonged
592 low oxygen exposure can impact on adaptation to chronic infection and providing insights into the
593 differences between short-term responses and long-term adaptation. Overall, we confirm that
594 hypoxia contributes to multiple phenotypic changes that are prevalent in chronic infection, opening
595 a path towards designing therapies targeting these.

596

597

598 # Materials and methods

599 ## Bacterial strains

600 *Pseudomonas aeruginosa* AMT 0023-30 early infection clinical isolate (E) and AMT 0023-31 late
601 infection clinical isolate (L) are two well characterised strains in the International *P. aeruginosa* panel
602 (30). Hypoxia- and normoxia-adapted *P. aeruginosa* strains were obtained in this study as described
603 below and are referred to as H1, H2, H3, N1, N2, and N3 (Table 1). If not stated otherwise, bacteria
604 were routinely grown in LB broth (Sigma-Aldrich, St. Louis, MO, USA) at 37°C with orbital agitation
605 (200 rpm) or plated on LB agar (Sigma-Aldrich, St. Louis, MO, USA) and grown at 37°C.

606 ## Experimental evolution

607 Overnight cultures of *P. aeruginosa* strain AMT 0023-30 (E) were inoculated into 30 ml LB media to
608 OD_{600} ~0.1. Prior to use, the media was equilibrated for 18 h at 37°C in an O_2 Control InVitro Glove
609 Box (PHGB model, Coy Laboratory Products, MI, United States) in 6% O_2, 5% CO_2 or in a Steri-Cycle
610 CO_2 Incubator (model 371, Thermo Scientific, Waltham, MA, USA) at 21% O_2, 5% CO_2. Three flasks
611 were inoculated for each of the conditions being examined. Additionally, aliquots (2 ml) of the
612 overnight *P. aeruginosa* cultures were retained as a controls for proteomic and transcriptomic
613 analysis. All flasks were incubated for 24h with agitation (200 rpm, CO_2 resistant orbital shaker, model
614 15351105, Thermo Fisher Scientific, Waltham, MA, USA) in hypoxic and normoxic conditions. Daily
615 aliquots (2 ml) were removed for proteomic analysis from each of the flasks and also additional
616 aliquots for OD_{600} measurements and plating. Glycerol stocks (50%, LB (v/v)) were prepared for
617 subsequent phenotype analysis and frozen immediately to ensure minimal oxygen exposure. A
618 volume of 5% of the bacterial culture was also transferred into 30 ml of pre-adapted media each day
619 and this procedure was continued for up to 28 days to determine long-term adaptation patterns. To
620 ensure stability of the hypoxic conditions, all of the samples from H1, H2 and H3 were taken inside

621 the hypoxia chamber. To ensure that there were no other environmental differences between the test
622 conditions other than oxygen levels, the same batch of media was used for both normoxia-adapting
623 and hypoxia-adapting flasks and shaking.

624 Whole proteome analysis

625 Samples (2 ml) were collected throughout the experimental evolution for proteome analysis. Bacterial
626 cells were pelleted at 14000-16000 g for 2 min and stored at -80ºC until further analysis. Whole cell
627 lysates were extracted from each of the hypoxia- and normoxia exposed cultures by resuspending in
628 1 ml of ice-cold lysis buffer containing 40mM Tris-HCl (pH 7.8) and 1x cOmplete™, EDTA-free protease
629 inhibitor cocktail (Roche, Basel, Switzerland). Cells were disrupted by a sonication with a sonic
630 dismembrator and microtip 6mm probe (model 505; Fisherbrand, Thermo Fisher Scientific, Waltham,
631 MA, USA) (set with 20% output power using eight 10 s bursts on ice). Cell debris and any remaining
632 intact cells were pelleted using centrifugation (12000 g for 30 min). Supernatants were transferred
633 into fresh tubes and the proteins were precipitated with four volumes of methanol and incubated in
634 -80ºC overnight. The samples were centrifuged at 12000 g for 30 min at 4ºC, supernatants
635 were removed, and the protein pellets were resuspended in 200 µl of resuspension buffer containing
636 8 M urea, 50 mM Tris-HCL (pH 8.0), before 1 M 1,4-dithiothreitol (DTT) was added to each supernatant
637 (10 µl/ml lysate) and incubated at 56ºC for 30 min, followed by the addition of 1 M iodoacetamide
638 (55 µl/ml lysate) which was incubated in darkness at room temperature for 20 min. Lysates were
639 dialyzed in SnakeSkin™ tubing (Thermo Fisher Scientific, Waltham, MA, USA) with a cut-off of 3.5 kDa
640 against 100 mM ammonium bicarbonate overnight, with stirring at 4ºC, followed by at least 4 more
641 hours incubation with fresh volumes of ammonium bicarbonate. Trypsin (400 ng/µl) (Sigma-Aldrich,
642 St. Louis, MO, USA) was added to the dialyzed protein (5 µl /100 µl protein) and tubes were incubated
643 overnight at 37ºC. Aliquots from each sample were placed in fresh tubes and samples were dried in a
644 vacufuge concentrator system (model 5301; Eppendorf, Hamburg, Germany) at 65ºC and

645 resuspended in 20 µl of ZipTips resuspension buffer containing 0.5% trifluoroacetic acid (TFA) in MilliQ
646 water. ZipTips (Merc Millipore, Burlington, MA, USA) were used for peptide purification as per the
647 manufacturers' instructions. Nanodrop spectrophotometer DS-11+ (DeNovix, Wilmington, DE, USA)
648 was used for peptide concentration measurements. The samples were analysed on a Bruker TimsTOF
649 Pro mass spectrometer connected to a Evosep One chromatography system. Peptides were separated
650 on an 8 cm analytical C18 column (Evosep, 3 µm beads, 100 µm ID) using the pre-set 33 samples per
651 day gradient on the Evosep one. A trapped ion mobility (TIMS) analyser was synchronized with a
652 quadrupole mass filter to enable the highly efficient PASEF (Parallel Accumulation Serial
653 Fragmentation acquisition) procedure with acquisition rates of 100 Hz. The accumulation and ramp
654 times for the TIMS were both set to 100 ms., with an ion mobility (1/k0) range from 0.62 to 1.46
655 Vs/cm. Spectra were recorded in the mass range from 100 to 1,700 m/z. The precursor (MS) Intensity
656 Threshold was set to 2,500 and the precursor Target Intensity set to 20,000. Each PASEF cycle
657 consisted of one MS ramp for precursor detection followed by 10 PASEF MS/MS ramps, with a total
658 cycle time of 1.16 s.

659 Protein identification and label-free quantitative (LFQ) analysis was conducted using MaxQuant (v
660 2.4.2.0, https://maxquant.org/) by searching against the reference strain *P. aeruginosa* PAO1 (ATCC
661 15692). For protein identification, the following search parameters were used: trypsin was the
662 digesting enzyme with up to two missed cleavages allowed for; oxidation on methionine and
663 acetylation on the N terminus were selected as variable modifications with a fixed modification of
664 carbamidylation on cysteine; Label Free Quantitation (LFQ) and Match Between Runs (MBR) options
665 were selected. FDR for protein and peptide were set at 1%.

666 One sample from each 28 day culture was analysed, with one technical replicate for a randomly
667 chosen sample and LFQ intensities were compared. All missing LFQ intensities were imputed with a
668 fixed value of 1. The mean was calculated separately for the hypoxia and normoxia samples, followed

669 by fold change (FC) calculation. T-test statistical analysis was performed to identify proteins with a
670 significantly changed abundance (p-value ≤ 0.05). Proteins with a -1.5 ≤ FC ≥ 1.5 were considered.

671 Antibiotic resistance

672 Overnight bacterial cultures were diluted in 10 ml of fresh LB to OD_{600} equal to 0.1. Bacteria were
673 spread evenly on Mueller–Hinton agar plates (Neogen, Lansing, MI, USA) using cotton swabs, in three
674 directions, to give a homogenous lawn. Antibiotic disks (Oxoid, Hampshire, UK) were placed on the
675 surface of the agar and the plates were incubated overnight in normoxic conditions at 37ºC. Growth
676 inhibition zone diameters were measured in at least two points, and the mean was used for statistical
677 analysis.

678 Motility

679 Motility assays were performed as describe by Rashid & Kornberg (2000). Swimming motility was
680 assessed by inoculating the surface of a 0.3 % (w/v) LB agar plate with overnight culture using a sterile
681 toothpick. Swimming and swarming plates were incubated overnight in normoxic conditions at 37ºC
682 for ~18 h. For swarming motility 0.8% nutrient broth (Sigma-Aldrich, St. Louis, MO, USA), 0.5%
683 dextrose, 0.5% agar plates were inoculated identically as for swimming motility assessment. The
684 diameter of bacterial growth zones was measured in at least two directions, and the mean was used
685 for statistical analysis. Twitching motility was assessed by inoculating 1.5 % (w/v) LB agar plate by
686 piercing through the agar. Plates were incubated overnight in normoxic conditions at 37ºC for ~18 h,
687 and the agar was removed. Bacteria on the surface of the plate were stained with 1% (w/v) crystal
688 violet for 20 min. The plates were washed with water until all excess dye was removed and dried at
689 room temperature. The diameter of the growth zone was measured in at least two points, and the
690 mean was used for statistical analysis.

691 ## Biofilm production

692 Overnight cultures of PA strains were diluted in fresh LB media to OD_{600} of ~0.1, and 100 µl of each
693 diluted culture was transferred into 6 wells of a 96-well plate. The plates were incubated statically in
694 normoxic conditions at 37°C for 24, 48 or 72 h and OD_{600} was measured with the Synergy H1
695 microplate reader (Mason Technology, Dublin, Ireland). The medium with planktonic bacteria was
696 removed, and the biofilm fixed by incubation with 200ul of methanol for 10 min. The wells were
697 washed three times with phosphate buffered saline (PBS) (Sigma-Aldrich, St. Louis, MO, USA),
698 followed by the addition of 200 µl of 0.1% crystal violet solution and 30 min incubation at room
699 temperature. The solution was removed, and the wells were washed three times with water and once
700 with PBS. The plates were dried for at least 30 min at room temperature and 150 µl of 96% ethanol
701 was added to dissolve the bound stain. After 10 min of incubation at room temperature, the solution
702 was mixed by pipetting, OD_{590} was determined, and the OD_{590}/OD_{600} ratio was calculated.

703 ## Exopolysaccharide production - Congo Red agar assay

704 Overnight cultures of PA strains were pelleted and washed with 1 ml of PBS. The pellets were
705 resuspended in PBS to OD_{600} of ~0.1 and 1 µl of the suspension was plated on a Congo Red agar plate
706 (10 g/L Tryptone, 10 g/ L Bactoagar, 40mg/L Congo Red, 20mg/L Coomassie Brilliant Blue). The plates
707 were incubated for 48 h in normoxic conditions and colony morphology was assessed.

708 ## Stress sensitivity assays

709 Overnight cultures of PA strains were diluted to a CFU/ml of 10^8 and a range of serial dilutions was
710 prepared. Suspensions (1ul) were plated on one of the following: LB agar control plates, LB agar
711 supplemented with 0.5 M NaCl (osmotic stress), LB agar supplemented with 1mM H_2O_2 (oxidative
712 stress), or LB agar, pH 5 (acidic stress). The plates were incubated in normoxic conditions at 37°C for

713 24 or 48 h. Temperature stress was determined by incubation of an LB agar plate at 45°C for 24 h.
714 Change of sensitivity was determined by determining the lowest dilution at which bacterial growth
715 was observed.

716 *Galleria mellonella* infection model

717 Virulence was determined as previously described (32). Wax moth larvae (*Galleria mellonella*) (The
718 KammieShop, Waalwijk, Denmark) were equilibrated in normoxic conditions at 15°C for at least 7 days
719 after arrival and stored at the same conditions for up to 4 weeks, during which larvae with a weight
720 range of 0.2-0.4 g were selected for experiments. Overnight bacterial cultures in LB were diluted in
721 fresh media to OD_{600} of ~0.1 and grown for 2-3 h. Cultures were centrifuged, and bacterial cells were
722 washed with PBS. The bacteria were diluted to 10^6 CFU/ml and serially diluted to 10^{-6}. Each dilution
723 was injected (20 µl) into the hindmost left proleg of healthy larvae (10 per group) and the same
724 volume of PBS was injected into one group as a control. Injected larvae were incubated at 37°C for
725 72 h and the number of cells causing an LD_{50} after 24 h was determined through bioburden
726 assessment by plating bacteria onto LB agar and counting colonies after 24 h.

727 Pyocyanin production quantification

728 *P. aeruginosa* strains were inoculated to OD_{600} in fresh PB media (20g/L Bacto-Peptone, 1.4g/L $MgCl_2$,
729 10g/L K_2SO_4) and cultured with aeration in normoxic conditions at 37°C to maximize pyocyanin
730 production. The bacterial cultures were pelleted (10 min at 12300 g) and two 7.5-ml replicates were
731 withdrawn from each of the 18 h stationary phase cultures. Pyocyanin was extracted with 4.5 ml of
732 chloroform and a total of 1.5 ml of 0.2 M HCl was added to each extract causing colour change from
733 blue to pink. The absorbance of this solution was measured at 520 nm, and the obtained values were
734 converted to pyocyanin content following Essar et al. (1990) (139). The experiment was repeated at
735 least two times.

736 ## Automatic growth curves

737 To assess the influence of the inoculation volume on the growth patterns of *P. aeruginosa* AMT 0023-
738 30, 24h stationary phase cultures were inoculated into fresh LB media in a way they constituted 1%,
739 5% or 10% of the new culture. Three 200 µl technical replicates of the cultures were transferred into
740 a 96-well plate and incubated in normoxic conditions at 37°C with agitation.

741 ## Growth curves

742 To assess the differences in the numbers of generations in hypoxic conditions and normoxic
743 conditions of the AMT0063-30 early infection strain overnight cultures were prepared. The following
744 day they were inoculated in triplicate into fresh LB media and incubated with aeration at 37°C in the
745 O_2 Control InVitro Glove Box in 6% O_2, 5% CO_2 or in 21% O_2, 5% CO_2 or in the Steri-Cycle CO_2 Incubator
746 at 21% O_2, 5% CO_2. Every hour a sample was taken from each culture for OD_{600} measurements and
747 plating on LB agar. The agar plates were incubated overnight at 37°C and the colony forming units
748 were calculated and OD_{600} to CFU/ml was plotted, a trend line was determined and R^2 calculated. The
749 doubling time was calculated for the logarithmic phase of growth using the following formula:
750 Doubling time = (Duration (min)**ln*(2))/[*ln*(final cell concentration/initial cell concentration)].

751 # Acknowledgements

752 JD, CJC are supported by an SFI Frontiers of the Future award (20/FFP-P/8717) to SMcC. ND was
753 supported by the Irish Research Council, GOIPG/2021/1443 IRC Award. The authors are grateful to Dr
754 David Gomez-Matallanas for his advice in proteomic analysis and for the support of the staff and
755 facilities in the UCD Conway proteomics core.

756

References

1. Antimicrobial resistance collaborators. Antimicrobial Resistance Collaborators: Global burden of bacterial antimicrobial resistance in 2019: a systematic analysis. Lancet. 2022 Feb 12;399(10325):629–55.

2. O'Neill J. Tackling drug-resistant infections globally: final report and recommendations [Internet]. 2016 May [cited 2024 Oct 4]. Available from: https://wellcomecollection.org/works/thvwsuba

3. Blanchard AC, Waters VJ. Opportunistic Pathogens in Cystic Fibrosis: Epidemiology and Pathogenesis of Lung Infection. Journal of the Pediatric Infectious Diseases Society. 2022 Sep 1;11(Supplement_2):S3–12.

4. Sanz-García F, Gil-Gil T, Laborda P, Ochoa-Sánchez LE, Martínez JL, Hernando-Amado S. Coming from the Wild: Multidrug Resistant Opportunistic Pathogens Presenting a Primary, Not Human-Linked, Environmental Habitat. International Journal of Molecular Sciences. 2021 Jan;22(15):8080.

5. Serra-Burriel M, Keys M, Campillo-Artero C, Agodi A, Barchitta M, Gikas A, et al. Impact of multi-drug resistant bacteria on economic and clinical outcomes of healthcare-associated infections in adults: Systematic review and meta-analysis. PLoS One. 2020;15(1):e0227139.

6. Reynolds D, Kollef M. The Epidemiology and Pathogenesis and Treatment of Pseudomonas aeruginosa Infections: An Update. Drugs. 2021 Dec 1;81(18):2117–31.

7. Li Y, Roberts JA, Walker MM, Aslan AT, Harris PNA, Sime FB. The global epidemiology of ventilator-associated pneumonia caused by multi-drug resistant *Pseudomonas aeruginosa*: A systematic review and meta-analysis. International Journal of Infectious Diseases. 2024 Feb 1;139:78–85.

8. Rossi E, La Rosa R, Bartell JA, Marvig RL, Haagensen JAJ, Sommer LM, et al. Pseudomonas aeruginosa adaptation and evolution in patients with cystic fibrosis. Nat Rev Microbiol. 2021 May;19(5):331–42.

9. Smith WD, Bardin E, Cameron L, Edmondson CL, Farrant KV, Martin I, et al. Current and future therapies for Pseudomonas aeruginosa infection in patients with cystic fibrosis. FEMS Microbiology Letters. 2017 Aug 1;364(14):fnx121.

10. Botelho J, Grosso F, Peixe L. Antibiotic resistance in *Pseudomonas aeruginosa* – Mechanisms, epidemiology and evolution. Drug Resistance Updates. 2019 May 1;44:100640.

11. Bakkeren E, Diard M, Hardt WD. Evolutionary causes and consequences of bacterial antibiotic persistence. Nat Rev Microbiol. 2020 Sep;18(9):479–90.

12. Sett A, Dubey V, Bhowmik S, Pathania R. Decoding Bacterial Persistence: Mechanisms and Strategies for Effective Eradication. ACS Infect Dis [Internet]. 2024 Jun 28 [cited 2024 Jul 1]; Available from: https://doi.org/10.1021/acsinfecdis.4c00270

13. ECDC. Healthcare-associated infections acquired in intensive care units - Annual Epidemiological Report for 2016 [Internet]. Stockholm; 2018 [cited 2024 May 15]. Available from: https://www.ecdc.europa.eu/en/publications-data/healthcare-associated-infections-intensive-care-units-2019

14. ECDC. Healthcare-associated infections acquired in intensive care units - Annual Epidemiological Report for 2019 [Internet]. Stockholm; 2023 [cited 2024 May 15]. Available from: https://www.ecdc.europa.eu/en/publications-data/healthcare-associated-infections-intensive-care-units-2019

15. Tacconelli E, Carrara E, Savoldi A, Harbarth S, Mendelson M, Monnet DL, et al. Discovery, research, and development of new antibiotics: the WHO priority list of antibiotic-resistant bacteria and tuberculosis. The Lancet Infectious Diseases. 2018 Mar 1;18(3):318–27.

16. WHO. WHO bacterial priority pathogens list, 2024: Bacterial pathogens of public health importance to guide research, development and strategies to prevent and control antimicrobial resistance [Internet]. 2024 [cited 2024 Dec 5]. Available from: https://www.who.int/publications/i/item/9789240093461

17. Cullen L, McClean S. Bacterial Adaptation during Chronic Respiratory Infections. Pathogens. 2015 Mar;4(1):66–89.

18. Jurado-Martín I, Sainz-Mejías M, McClean S. Pseudomonas aeruginosa: An Audacious Pathogen with an Adaptable Arsenal of Virulence Factors. Int J Mol Sci. 2021 Mar 18;22(6):3128.

19. Moradali MF, Ghods S, Rehm BHA. Pseudomonas aeruginosa Lifestyle: A Paradigm for Adaptation, Survival, and Persistence. Front Cell Infect Microbiol [Internet]. 2017 Feb 15 [cited 2024 Jul 1];7. Available from: https://www.frontiersin.org/journals/cellular-and-infection-microbiology/articles/10.3389/fcimb.2017.00039/full

20. Camus L, Vandenesch F, Moreau K. From genotype to phenotype: adaptations of Pseudomonas aeruginosa to the cystic fibrosis environment. Microbial Genomics. 2021;7(3):000513.

21. Chadha J, Harjai K, Chhibber S. Revisiting the virulence hallmarks of Pseudomonas aeruginosa: a chronicle through the perspective of quorum sensing. Environmental Microbiology. 2022;24(6):2630–56.

22. Cramer N, Klockgether J, Tümmler B. Microevolution of Pseudomonas aeruginosa in the airways of people with cystic fibrosis. Current Opinion in Immunology. 2023 Aug 1;83:102328.

23. Rosales-Reyes R, Vargas-Roldán SY, Lezana-Fernández JL, Santos-Preciado JI. *Pseudomonas Aeruginosa*: Genetic Adaptation, A Strategy for its Persistence in Cystic Fibrosis. Archives of Medical Research. 2021 May 1;52(4):357–61.

24. Worlitzsch D, Tarran R, Ulrich M, Schwab U, Cekici A, Meyer KC, et al. Effects of reduced mucus oxygen concentration in airway Pseudomonas infections of cystic fibrosis patients. J Clin Invest. 2002 Feb;109(3):317–25.

25. Alvarez-Ortega C, Harwood CS. Responses of Pseudomonas aeruginosa to low oxygen indicate that growth in the cystic fibrosis lung is by aerobic respiration. Molecular Microbiology. 2007;65(1):153–65.

26. Hassett DJ, Sutton MD, Schurr MJ, Herr AB, Caldwell CC, Matu JO. </i>Pseudomonas aeruginosa</i> hypoxic or anaerobic biofilm infections within cystic fibrosis airways. Trends in Microbiology. 2009 Mar 1;17(3):130–8.

27. Cullen L, O'Connor A, McCormack S, Owens RA, Holt GS, Collins C, et al. The involvement of the low-oxygen-activated locus of Burkholderia cenocepacia in adaptation during cystic fibrosis infection. Sci Rep. 2018 Sep 6;8(1):13386.

28. O'Connor A, Jurado-Martín I, Mysior MM, Manzira AL, Drabinska J, Simpson JC, et al. A universal stress protein upregulated by hypoxia has a role in Burkholderia cenocepacia intramacrophage survival: Implications for chronic infection in cystic fibrosis. Microbiologyopen. 2022 Dec 9;12(1):e1311.

29. Mulcahy LR, Burns JL, Lory S, Lewis K. Emergence of Pseudomonas aeruginosa Strains Producing High Levels of Persister Cells in Patients with Cystic Fibrosis. Journal of Bacteriology. 2010 Oct 8;192(23):6191.

30. De Soyza A, Hall AJ, Mahenthiralingam E, Drevinek P, Kaca W, Drulis-Kawa Z, et al. Developing an international Pseudomonas aeruginosa reference panel. Microbiologyopen. 2013 Dec;2(6):1010–23.

31. Freschi L, Bertelli C, Jeukens J, Moore MP, Kukavica-Ibrulj I, Emond-Rheault JG, et al. Genomic characterisation of an international Pseudomonas aeruginosa reference panel indicates that the two major groups draw upon distinct mobile gene pools. FEMS Microbiol Lett. 2018 Jul 1;365(14).

32. Cullen L, Weiser R, Olszak T, Maldonado RF, Moreira AS, Slachmuylders L, et al. Phenotypic characterization of an international Pseudomonas aeruginosa reference panel: strains of cystic fibrosis (CF) origin show less in vivo virulence than non-CF strains. Microbiology. 2015;161(10):1961–77.

33. Aanaes K, Rickelt LF, Johansen HK, von Buchwald C, Pressler T, Høiby N, et al. Decreased mucosal oxygen tension in the maxillary sinuses in patients with cystic fibrosis. J Cyst Fibros. 2011 Mar;10(2):114–20.

34. Walkiewicz A, Brzezińska M, Bieganowski A. Methanotrophs are favored under hypoxia in ammonium-fertilized soils. Biol Fertil Soils. 2018 Oct 1;54(7):861–70.

35. Xu A, Zhang X, Wang T, Xin F, Ma LZ, Zhou J, et al. Rugose small colony variant and its hyper-biofilm in *Pseudomonas aeruginosa*: Adaption, evolution, and biotechnological potential. Biotechnology Advances. 2021 Dec 1;53:107862.

36. Marmont LS, Rich JD, Whitney JC, Whitfield GB, Almblad H, Robinson H, et al. Oligomeric lipoprotein PelC guides Pel polysaccharide export across the outer membrane of Pseudomonas aeruginosa. Proceedings of the National Academy of Sciences. 2017 Mar 14;114(11):2892–7.

37. Poudyal B, Sauer K. The ABC of Biofilm Drug Tolerance: the MerR-Like Regulator BrlR Is an Activator of ABC Transport Systems, with PA1874-77 Contributing to the Tolerance of Pseudomonas aeruginosa Biofilms to Tobramycin. Antimicrobial Agents and Chemotherapy. 2018 Jan 25;62(2):10.1128/aac.01981-17.

871 38. Avila-Cobian LF, De Benedetti S, Kim C, Feltzer R, Champion MM, Fisher JF, et al. In vitro studies
872 of the protein-interaction network of cell-wall lytic transglycosylase RlpA of Pseudomonas
873 aeruginosa. Commun Biol. 2022 Nov 30;5(1):1–16.

874 39. Benkert B, Quäck N, Schreiber K, Jaensch L, Jahn D, Schobert M. Nitrate-responsive NarX-NarL
875 represses arginine-mediated induction of the Pseudomonas aeruginosa arginine fermentation
876 arcDABC operon. Microbiology. 2008;154(10):3053–60.

877 40. Schreiber K, Krieger R, Benkert B, Eschbach M, Arai H, Schobert M, et al. The Anaerobic
878 Regulatory Network Required for Pseudomonas aeruginosa Nitrate Respiration. Journal of
879 Bacteriology. 2007 Jun;189(11):4310–4.

880 41. Raba DA, Yuan M, Fang X, Menzer WM, Xie B, Liang P, et al. Role of Subunit D in Ubiquinone-
881 Binding Site of Vibrio cholerae NQR: Pocket Flexibility and Inhibitor Resistance. ACS Omega. 2019
882 Nov 19;4(21):19324–31.

883 42. Kotecka K, Kawalek A, Kobylecki K, Bartosik AA. The MarR-Type Regulator PA3458 Is Involved in
884 Osmoadaptation Control in Pseudomonas aeruginosa. International Journal of Molecular
885 Sciences. 2021 Jan;22(8):3982.

886 43. Aspedon A, Palmer K, Whiteley M. Microarray Analysis of the Osmotic Stress Response in
887 Pseudomonas aeruginosa. J Bacteriol. 2006 Apr;188(7):2721–5.

888 44. Wood LF, Ohman DE. Identification of Genes in the σ22 Regulon of Pseudomonas aeruginosa
889 Required for Cell Envelope Homeostasis in Either the Planktonic or the Sessile Mode of Growth.
890 mBio. 2012 May 15;3(3):10.1128/mbio.00094-12.

891 45. D'Souza-Ault MR, Smith LT, Smith GM. Roles of N-acetylglutaminylglutamine amide and glycine
892 betaine in adaptation of Pseudomonas aeruginosa to osmotic stress. Appl Environ Microbiol.
893 1993 Feb;59(2):473–8.

894 46. Delden C van, Page MGP, Köhler T. Involvement of Fe Uptake Systems and AmpC β-Lactamase in
895 Susceptibility to the Siderophore Monosulfactam BAL30072 in Pseudomonas aeruginosa.
896 Antimicrobial Agents and Chemotherapy. 2013 May;57(5):2095.

897 47. Déziel E, Gopalan S, Tampakaki AP, Lépine F, Padfield KE, Saucier M, et al. The contribution of
898 MvfR to Pseudomonas aeruginosa pathogenesis and quorum sensing circuitry regulation:
899 multiple quorum sensing-regulated genes are modulated without affecting lasRI, rhlRI or the
900 production of N-acyl- l-homoserine lactones. Molecular Microbiology. 2005;55(4):998–1014.

901 48. Irons JL, Hodge-Hanson K, Downs DM. RidA Proteins Protect against Metabolic Damage by
902 Reactive Intermediates. Microbiology and Molecular Biology Reviews. 2020 Jul
903 15;84(3):10.1128/mmbr.00024-20.

904 49. Irons J, Hodge-Hanson KM, Downs DM. PA5339, a RidA Homolog, Is Required for Full Growth in
905 Pseudomonas aeruginosa. Journal of Bacteriology. 2018 Oct 23;200(22):10.1128/jb.00434-18.

906 50. Weiler AJ, Spitz O, Gudzuhn M, Schott-Verdugo SN, Kamel M, Thiele B, et al. A phospholipase B
907 from *Pseudomonas aeruginosa* with activity towards endogenous phospholipids affects biofilm
908 assembly. Biochimica et Biophysica Acta (BBA) - Molecular and Cell Biology of Lipids. 2022 Apr
909 1;1867(4):159101.

910 51. Yoon SS, Hennigan RF, Hilliard GM, Ochsner UA, Parvatiyar K, Kamani MC, et al. Pseudomonas
911 aeruginosa Anaerobic Respiration in Biofilms: Relationships to Cystic Fibrosis Pathogenesis.
912 Developmental Cell. 2002;

913 52. König J, Schreiber R, Voelcker T, Mall M, Kunzelmann K. The cystic fibrosis transmembrane
914 conductance regulator (CFTR) inhibits ENaC through an increase in the intracellular Cl–
915 concentration. EMBO Rep. 2001 Nov 15;2(11):1047–51.

916 53. Cowley ES, Kopf SH, LaRiviere A, Ziebis W, Newman DK. Pediatric Cystic Fibrosis Sputum Can Be
917 Chemically Dynamic, Anoxic, and Extremely Reduced Due to Hydrogen Sulfide Formation. mBio.
918 2015 Jul 28;6(4):10.1128/mbio.00767-15.

919 54. Line L, Alhede M, Kolpen M, Kühl M, Ciofu O, Bjarnsholt T, et al. Physiological levels of nitrate
920 support anoxic growth by denitrification of Pseudomonas aeruginosa at growth rates reported
921 in cystic fibrosis lungs and sputum. Front Microbiol. 2014 Oct 24;5:554.

922 55. Borriello G, Richards L, Ehrlich GD, Stewart PS. Arginine or Nitrate Enhances Antibiotic
923 Susceptibility of Pseudomonas aeruginosa in Biofilms. Antimicrobial Agents and Chemotherapy.
924 2006 Jan;50(1):382–4.

925 56. Tribelli PM, Lujan AM, Pardo A, Ibarra JG, Fernández Do Porto D, Smania A, et al. Core regulon
926 of the global anaerobic regulator Anr targets central metabolism functions in Pseudomonas
927 species. Sci Rep. 2019 Jun 21;9(1):9065.

928 57. Trunk K, Benkert B, Quäck N, Münch R, Scheer M, Garbe J, et al. Anaerobic adaptation in
929 Pseudomonas aeruginosa: definition of the Anr and Dnr regulons. Environmental Microbiology.
930 2010;12(6):1719–33.

931 58. Ashish A, Paterson S, Mowat E, Fothergill JL, Walshaw MJ, Winstanley C. Extensive diversification
932 is a common feature of Pseudomonas aeruginosa populations during respiratory infections in
933 cystic fibrosis. J Cyst Fibros. 2013 Dec;12(6):790–3.

934 59. Flynn KM, Dowell G, Johnson TM, Koestler BJ, Waters CM, Cooper VS. Evolution of Ecological
935 Diversity in Biofilms of Pseudomonas aeruginosa by Altered Cyclic Diguanylate Signaling. Journal
936 of Bacteriology. 2016 Sep 9;198(19):2608–18.

937 60. Jorth P, Staudinger BJ, Wu X, Hisert K, Hayden H, Garudathri J, et al. Regional Isolation Drives
938 Bacterial Diversification within Cystic Fibrosis Lungs. Cell Host Microbe. 2015 Sep 9;18(3):307–
939 19.

940 61. Markussen T, Marvig RL, Gómez-Lozano M, Aanæs K, Burleigh AE, Høiby N, et al. Environmental
941 heterogeneity drives within-host diversification and evolution of Pseudomonas aeruginosa.
942 mBio. 2014 Sep 16;5(5):e01592-01514.

943 62. Winstanley C, O'Brien S, Brockhurst MA. Pseudomonas aeruginosa Evolutionary Adaptation and
944 Diversification in Cystic Fibrosis Chronic Lung Infections. Trends Microbiol. 2016 May;24(5):327–
945 37.

946 63. Kamath KS, Krisp C, Chick J, Pascovici D, Gygi SP, Molloy MP. Pseudomonas aeruginosa Proteome
947 under Hypoxic Stress Conditions Mimicking the Cystic Fibrosis Lung. J Proteome Res. 2017 Oct
948 6;16(10):3917–28.

949 64. Sommer LM, Johansen HK, Molin S. Antibiotic resistance in Pseudomonas aeruginosa and
950 adaptation to complex dynamic environments. Microbial Genomics. 2020;6(5):e000370.

951 65. Besse A, Groleau MC, Trottier M, Vincent AT, Déziel E. Pseudomonas aeruginosa Strains from
952 Both Clinical and Environmental Origins Readily Adopt a Stable Small-Colony-Variant Phenotype
953 Resulting from Single Mutations in c-di-GMP Pathways. J Bacteriol. 2022 Oct
954 18;204(10):e0018522.

955 66. Johns BE, Purdy KJ, Tucker NP, Maddocks SE. Phenotypic and Genotypic Characteristics of Small
956 Colony Variants and Their Role in Chronic Infection. Microbiol Insights. 2015 Jan 1;8:MBI.S25800.

957 67. Ryan H, Ballard E, Stockwell RE, Duplancic C, Thomson RM, Smith K, et al. A systematic review of
958 the clinical impact of small colony variants in patients with cystic fibrosis. BMC Pulm Med. 2023
959 Sep 1;23(1):323.

960 68. Schneider M, Mühlemann K, Droz S, Couzinet S, Casaulta C, Zimmerli S. Clinical Characteristics
961 Associated with Isolation of Small-Colony Variants of Staphylococcus aureus and Pseudomonas
962 aeruginosa from Respiratory Secretions of Patients with Cystic Fibrosis. Journal of Clinical
963 Microbiology. 2008 Mar 5;46(5):1832.

964 69. Malone JG. Role of small colony variants in persistence of Pseudomonas aeruginosa infections
965 in cystic fibrosis lungs. Infection and Drug Resistance. 2015 Jul 29;8(null):237–47.

966 70. Besse A, Groleau MC, Déziel E. Emergence of Small Colony Variants Is an Adaptive Strategy Used
967 by Pseudomonas aeruginosa to Mitigate the Effects of Redox Imbalance. mSphere. 2023 Feb
968 28;8(2):e00057-23.

969 71. Hoffman LR, Déziel E, D'Argenio DA, Lépine F, Emerson J, McNamara S, et al. Selection for
970 Staphylococcus aureus small-colony variants due to growth in the presence of Pseudomonas
971 aeruginosa. Proceedings of the National Academy of Sciences. 2006 Dec 26;103(52):19890–5.

972 72. Bjarnsholt T, Jensen PØ, Fiandaca MJ, Pedersen J, Hansen CR, Andersen CB, et al. Pseudomonas
973 aeruginosa biofilms in the respiratory tract of cystic fibrosis patients. Pediatr Pulmonol. 2009
974 Jun;44(6):547–58.

975 73. Høiby N, Ciofu O, Bjarnsholt T. Pseudomonas Aeruginosa Biofilms in Cystic fibrosis. Future
976 Microbiology. 2010 Nov 1;5(11):1663–74.

977 74. Maurice NM, Bedi B, Sadikot RT. Pseudomonas aeruginosa Biofilms: Host Response and Clinical
978 Implications in Lung Infections. Am J Respir Cell Mol Biol. 2018 Apr;58(4):428–39.

979 75. Klementiev AD, Jin Z, Whiteley M. Micron Scale Spatial Measurement of the O2 Gradient
980 Surrounding a Bacterial Biofilm in Real Time. mBio. 2020 Oct 20;11(5):10.1128/mbio.02536-20.

981 76. Wu Y, Klapper I, Stewart PS. Hypoxia arising from concerted oxygen consumption by neutrophils
982 and microorganisms in biofilms. Pathogens and Disease. 2018 Apr 23;76(4):fty043.

983 77. Bowler P, Murphy C, Wolcott R. Biofilm exacerbates antibiotic resistance: Is this a current
984 oversight in antimicrobial stewardship? Antimicrob Resist Infect Control. 2020 Oct 20;9(1):162.

985 78. Liang Z, Nilsson M, Kragh KN, Hedal I, Alcàcer-Almansa J, Kiilerich RO, et al. The role of individual
986 exopolysaccharides in antibiotic tolerance of Pseudomonas aeruginosa aggregates. Front
987 Microbiol [Internet]. 2023 Jun 2 [cited 2024 Jul 2];14. Available from:
988 https://www.frontiersin.org/journals/microbiology/articles/10.3389/fmicb.2023.1187708/full

989 79. Caiazza NC, O'Toole GA. SadB is required for the transition from reversible to irreversible
990 attachment during biofilm formation by Pseudomonas aeruginosa PA14. J Bacteriol. 2004
991 Jul;186(14):4476–85.

992 80. Caiazza NC, Merritt JH, Brothers KM, O'Toole GA. Inverse Regulation of Biofilm Formation and
993 Swarming Motility by Pseudomonas aeruginosa PA14. J Bacteriol. 2007 May;189(9):3603–12.

994 81. Bazire A, Shioya K, Soum-Soutéra E, Bouffartigues E, Ryder C, Guentas-Dombrowsky L, et al. The
995 sigma factor AlgU plays a key role in formation of robust biofilms by nonmucoid Pseudomonas
996 aeruginosa. J Bacteriol. 2010 Jun;192(12):3001–10.

997 82. Candido Caçador N, Paulino da Costa Capizzani C, Gomes Monteiro Marin Torres LA, Galetti R,
998 Ciofu O, da Costa Darini AL, et al. Adaptation of Pseudomonas aeruginosa to the chronic
999 phenotype by mutations in the algTmucABD operon in isolates from Brazilian cystic fibrosis
1000 patients. PLoS One. 2018;13(11):e0208013.

1001 83. Hershberger CD, Ye RW, Parsek MR, Xie ZD, Chakrabarty AM. The algT (algU) gene of
1002 Pseudomonas aeruginosa, a key regulator involved in alginate biosynthesis, encodes an
1003 alternative sigma factor (sigma E). Proc Natl Acad Sci U S A. 1995 Aug 15;92(17):7941–5.

1004 84. Moscoso JA, Jaeger T, Valentini M, Hui K, Jenal U, Filloux A. The Diguanylate Cyclase SadC Is a
1005 Central Player in Gac/Rsm-Mediated Biofilm Formation in Pseudomonas aeruginosa. Journal of
1006 Bacteriology. 2014 Oct 29;196(23):4081–8.

1007 85. Schmidt A, Hammerbacher AS, Bastian M, Nieken KJ, Klockgether J, Merighi M, et al. Oxygen-
1008 dependent regulation of c-di-GMP synthesis by SadC controls alginate production in
1009 seudomonas aeruginosa. Environmental Microbiology. 2016;18(10):3390–402.

1010 86. Stacey SD, Pritchett CL. Pseudomonas aeruginosa AlgU Contributes to Posttranscriptional
1011 Activity by Increasing rsmA Expression in a mucA22 Strain. Journal of Bacteriology. 2016 Jun
1012 13;198(13):1812–26.

1013 87. Vijay-Kumar M, Gewirtz AT. Flagellin: key target of mucosal innate immunity. Mucosal
1014 Immunology. 2009 May 1;2(3):197–205.

1015 88. Neidig A, Yeung AT, Rosay T, Tettmann B, Strempel N, Rueger M, et al. TypA is involved in
1016 virulence, antimicrobial resistance and biofilm formation in Pseudomonas aeruginosa. BMC
1017 Microbiol. 2013 Apr 9;13(1):77.

1018 89. Overhage J, Lewenza S, Marr AK, Hancock REW. Identification of genes involved in swarming
1019 motility using a Pseudomonas aeruginosa PAO1 mini-Tn5-lux mutant library. J Bacteriol. 2007
1020 Mar;189(5):2164–9.

1021 90. Sindeldecker D, Stoodley P. The many antibiotic resistance and tolerance strategies of
1022 *Pseudomonas aeruginosa*. Biofilm. 2021 Dec 1;3:100056.

1023 91. Borriello G, Werner E, Roe F, Kim AM, Ehrlich GD, Stewart PS. Oxygen Limitation Contributes to
1024 Antibiotic Tolerance of Pseudomonas aeruginosa in Biofilms. Antimicrobial Agents and
1025 Chemotherapy. 2004 Jul;48(7):2659–64.

1026 92. Schaible B, Taylor CT, Schaffer K. Hypoxia Increases Antibiotic Resistance in Pseudomonas
1027 aeruginosa through Altering the Composition of Multidrug Efflux Pumps. Antimicrobial Agents
1028 and Chemotherapy. 2012 Mar 16;56(4):2114–8.

1029 93. Zhao X, Drlica K. Reactive oxygen species and the bacterial response to lethal stress. Current
1030 opinion in microbiology. 2014 Jul 30;0:1.

1031 94. Puchelle E, Bajolet O, Abély M. Airway mucus in cystic fibrosis. Paediatric Respiratory Reviews.
1032 2002 Jun 1;3(2):115–9.

1033 95. Bhagirath AY, Li Y, Somayajula D, Dadashi M, Badr S, Duan K. Cystic fibrosis lung environment and
1034 Pseudomonas aeruginosa infection. BMC Pulm Med. 2016 Dec 5;16:174.

1035 96. Lan L, Murray TS, Kazmierczak BI, He C. Pseudomonas aeruginosa OspR is an oxidative stress
1036 sensing regulator that affects pigment production, antibiotic resistance and dissemination
1037 during infection. Molecular Microbiology. 2010;75(1):76–91.

1038 97. Fraud S, Poole K. Oxidative Stress Induction of the MexXY Multidrug Efflux Genes and Promotion
1039 of Aminoglycoside Resistance Development in Pseudomonas aeruginosa. Antimicrobial Agents
1040 and Chemotherapy. 2011 Feb 24;55(3):1068–74.

1041 98. Mohamed FA, Shaker GH, Askoura MM. Oxidative Stress Influences Pseudomonas aeruginosa
1042 Susceptibility to Antibiotics and Reduces Its Pathogenesis in Host. Curr Microbiol. 2020 Mar
1043 1;77(3):479–90.

1044 99. Bojanovič K, D'Arrigo I, Long KS. Global Transcriptional Responses to Osmotic, Oxidative, and
1045 Imipenem Stress Conditions in Pseudomonas putida. Applied and Environmental Microbiology.
1046 2017 Mar 17;83(7):e03236.

1047 100. Dawan J, Ahn J. Bacterial Stress Responses as Potential Targets in Overcoming Antibiotic
1048 Resistance. Microorganisms. 2022 Jul;10(7):1385.

1049 101. Hunter RC, Asfour F, Dingemans J, Osuna BL, Samad T, Malfroot A, et al. Ferrous Iron Is a
1050 Significant Component of Bioavailable Iron in Cystic Fibrosis Airways. mBio. 2013 Aug
1051 20;4(4):10.1128/mbio.00557-13.

1052 102. Moreau-Marquis S, Bomberger JM, Anderson GG, Swiatecka-Urban A, Ye S, O'Toole GA, et al.
1053 The DeltaF508-CFTR mutation results in increased biofilm formation by Pseudomonas
1054 aeruginosa by increasing iron availability. Am J Physiol Lung Cell Mol Physiol. 2008
1055 Jul;295(1):L25-37.

1056 103. Schalk IJ, Perraud Q. and its multiple strategies to access iron. Environmental Microbiology.
1057 2023;25(4):811–31.

1058 104. Reid DW, Carroll V, O'May C, Champion A, Kirov SM. Increased airway iron as a potential factor
1059 in the persistence of Pseudomonas aeruginosa infection in cystic fibrosis. European Respiratory
1060 Journal. 2007 Aug 1;30(2):286–92.

1061 105. Konings AF, Martin LW, Sharples KJ, Roddam LF, Latham R, Reid DW, et al. Pseudomonas
1062 aeruginosa Uses Multiple Pathways To Acquire Iron during Chronic Infection in Cystic Fibrosis
1063 Lungs. Infection and Immunity. 2013 Jul 11;81(8):2697–704.

1064 106. Lo Sciuto A, D'Angelo F, Spinnato MC, Garcia PS, Genah S, Matteo C, et al. A molecular
1065 comparison of [Fe-S] cluster-based homeostasis in Escherichia coli and Pseudomonas
1066 aeruginosa. mBio. 2024 Oct 3;0(0):e01206-24.

1067 107. Py B, Barras F. Building Fe–S proteins: bacterial strategies. Nat Rev Microbiol. 2010 Jun;8(6):436–
1068 46.

1069 108. Romsang A, Duang-Nkern J, Leesukon P, Saninjuk K, Vattanaviboon P, Mongkolsuk S. The Iron-
1070 Sulphur Cluster Biosynthesis Regulator IscR Contributes to Iron Homeostasis and Resistance to
1071 Oxidants in Pseudomonas aeruginosa. PLOS ONE. 2014 sty;9(1):e86763.

1072 109. Frangipani E, Visaggio D, Heeb S, Kaever V, Cámara M, Visca P, et al. The Gac/Rsm and cyclic-di-
1073 GMP signalling networks coordinately regulate iron uptake in seudomonas aeruginosa.
1074 Environmental Microbiology. 2014;16(3):676–88.

1075 110. Banin E, Brady KM, Greenberg EP. Chelator-induced dispersal and killing of Pseudomonas
1076 aeruginosa cells in a biofilm. Appl Environ Microbiol. 2006 Mar;72(3):2064–9.

1077 111. Schaible B, Rodriguez J, Garcia A, von Kriegsheim A, McClean S, Hickey C, et al. Hypoxia Reduces
1078 the Pathogenicity of Pseudomonas aeruginosa by Decreasing the Expression of Multiple
1079 Virulence Factors. J Infect Dis. 2017 May 1;215(9):1459–67.

1080 112. Gil-Marqués ML, Pachón-Ibáñez ME, Pachón J, Smani Y. Effect of Hypoxia on the Pathogenesis of
1081 Acinetobacter baumannii and Pseudomonas aeruginosa In Vitro and in Murine Experimental
1082 Models of Infection. Infection and Immunity. 2018 Sep 21;86(10):10.1128/iai.00543-18.

1083 113. Schaible B, McClean S, Selfridge A, Broquet A, Asehnoune K, Taylor CT, et al. Hypoxia Modulates
1084 Infection of Epithelial Cells by Pseudomonas aeruginosa. PLOS ONE. 2013 Feb 13;8(2):e56491.

1085 114. Vilaplana L, Marco MP. Phenazines as potential biomarkers of Pseudomonas aeruginosa
1086 infections: synthesis regulation, pathogenesis and analytical methods for their detection. Anal
1087 Bioanal Chem. 2020 Sep 1;412(24):5897–912.

1088 115. Jiao H, Li F, Wang T, Yam JKH, Yang L, Liang H. The Pyocin Regulator PrtR Regulates Virulence
1089 Expression of Pseudomonas aeruginosa by Modulation of Gac/Rsm System and c-di-GMP
1090 Signaling Pathway. Infection and Immunity [Internet]. 2021 Jan 19 [cited 2024 Oct 23];89(2).
1091 Available from: https://journals.asm.org/doi/full/10.1128/iai.00602-20

1092 116. Weimann A, Dinan AM, Ruis C, Bernut A, Pont S, Brown K, et al. Evolution and host-specific
1093 adaptation of Pseudomonas aeruginosa. Science. 2024 Jul 5;385(6704):eadi0908.

1094 117. Aguirre-Ramírez M, Medina G, González-Valdez A, Grosso-Becerra V, Soberón-Chávez G. The
1095 Pseudomonas aeruginosa rmlBDAC operon, encoding dTDP-l-rhamnose biosynthetic enzymes,
1096 is regulated by the quorum-sensing transcriptional regulator RhlR and the alternative sigma
1097 factor σS. Microbiology. 2012;158(4):908–16.

1098 118. Rahim R, Burrows LL, Monteiro MA, Perry MB, Lam JS. Involvement of the rml locus in core
1099 oligosaccharide and O polysaccharide assembly in Pseudomonas aeruginosa. Microbiology.
1100 2000;146(11):2803–14.

1101 119. Koska M, Kordes A, Erdmann J, Willger SD, Thöming JG, Bähre H, et al. Distinct Long- and Short-
1102 Term Adaptive Mechanisms in Pseudomonas aeruginosa. Microbiology Spectrum. 2022 Nov
1103 14;10(6):e03043-22.

1104 120. McHugh JP, Rodríguez-Quiñones F, Abdul-Tehrani H, Svistunenko DA, Poole RK, Cooper CE, et al.
1105 Global Iron-dependent Gene Regulation in *Escherichia coli*. Journal of Biological Chemistry. 2003
1106 Aug 8;278(32):29478–86.

1107 121. Touati D. Iron and oxidative stress in bacteria. Arch Biochem Biophys. 2000 Jan 1;373(1):1–6.

1108 122. Zhang Y, Zhang X, Zhang H, He Q, Zhou Q, Su Z, et al. Responses of Soil Bacteria to Long-Term
1109 and Short-Term Cadmium Stress as Revealed by Microbial Community Analysis. Bull Environ
1110 Contam Toxicol. 2009 Mar 1;82(3):367–72.

1111 123. Krulwich TA, Sachs G, Padan E. Molecular aspects of bacterial pH sensing and homeostasis.
1112 Nature reviews Microbiology. 2011 Apr 5;9(5):330.

1113 124. Clay ME, Hammond JH, Zhong F, Chen X, Kowalski CH, Lee AJ, et al. Pseudomonas aeruginosa
1114 lasR mutant fitness in microoxia is supported by an Anr-regulated oxygen-binding hemerythrin.
1115 Proc Natl Acad Sci U S A. 2020 Feb 11;117(6):3167–73.

1116 125. Neville N, Roberge N, Ji X, Stephen P, Lu JL, Jia Z. A Dual-Specificity Inhibitor Targets
1117 Polyphosphate Kinase 1 and 2 Enzymes To Attenuate Virulence of Pseudomonas aeruginosa.
1118 mBio. 2021 Jun 15;12(3):e00592.

1119 126. Ortiz-Severín J, Varas M, Bravo-Toncio C, Guiliani N, Chávez FP. Multiple antibiotic susceptibility
1120 of polyphosphate kinase mutants (ppk1 and ppk2) from Pseudomonas aeruginosa PAO1 as
1121 revealed by global phenotypic analysis. biol res. 2015 Apr 25;48(1):22.

1122 127. Salunkhe P, Smart CHM, Morgan JAW, Panagea S, Walshaw MJ, Hart CA, et al. A Cystic Fibrosis
1123 Epidemic Strain of Pseudomonas aeruginosa Displays Enhanced Virulence and Antimicrobial
1124 Resistance. Journal of Bacteriology. 2005 Jul;187(14):4908–20.

1125 128. An S, Wu J, Zhang LH. Modulation of Pseudomonas aeruginosa Biofilm Dispersal by a Cyclic-Di-
1126 GMP Phosphodiesterase with a Putative Hypoxia-Sensing Domain. Appl Environ Microbiol. 2010
1127 Dec;76(24):8160–73.

1128 129. Feng Q, Zhou J, Zhang L, Fu Y, Yang L. Insights into the molecular basis of c-di-GMP signalling in
1129 Pseudomonas aeruginosa. Critical Reviews in Microbiology. 2024 Jan 2;50(1):20–38.

1130 130. Hickman JW, Harwood CS. Identification of FleQ from Pseudomonas aeruginosa as a c-di-GMP-
1131 responsive transcription factor. Mol Microbiol. 2008 Jul;69(2):376–89.

1132 131. Matsuyama BY, Krasteva PV, Baraquet C, Harwood CS, Sondermann H, Navarro MVAS.
1133 Mechanistic insights into c-di-GMP-dependent control of the biofilm regulator FleQ from
1134 Pseudomonas aeruginosa. Proc Natl Acad Sci U S A. 2016 Jan 12;113(2):E209-218.

132. Zhou T, Huang J, Liu Z, Lin Q, Xu Z, Zhang LH. The Two-Component System FleS/FleR Represses H1-T6SS via Cyclic di-GMP Signaling in Pseudomonas aeruginosa. Appl Environ Microbiol. 2022 Jan 25;88(2):e0165521.

133. Amoureux L, Bador J, Fardeheb S, Mabille C, Couchot C, Massip C, et al. Detection of Achromobacter xylosoxidans in Hospital, Domestic, and Outdoor Environmental Samples and Comparison with Human Clinical Isolates. Appl Environ Microbiol. 2013 Dec;79(23):7142–9.

134. Crone S, Vives-Flórez M, Kvich L, Saunders AM, Malone M, Nicolaisen MH, et al. The environmental occurrence of Pseudomonas aeruginosa. APMIS. 2020;128(3):220–31.

135. Honda JR, Virdi R, Chan ED. Global Environmental Nontuberculous Mycobacteria and Their Contemporaneous Man-Made and Natural Niches. Front Microbiol. 2018 Aug 30;9.

136. Honda JR, Virdi R, Chan ED. Global Environmental Nontuberculous Mycobacteria and Their Contemporaneous Man-Made and Natural Niches. Front Microbiol. 2018;9:2029.

137. Price CTD, Hanford HE, Al-Quadan T, Santic M, Shin CJ, Da'as MSJ, et al. Amoebae as training grounds for microbial pathogens. mBio. 2024 Jul 8;15(8):e00827-24.

138. Mullard A. 2023 FDA approvals. Nat Rev Drug Discov. 2024 Feb;23(2):88–95.

139. Essar DW, Eberly L, Hadero A, Crawford IP. Identification and characterization of genes for a second anthranilate synthase in Pseudomonas aeruginosa: interchangeability of the two anthranilate synthases and evolutionary implications. J Bacteriol. 1990 Feb;172(2):884–900.

140. Ge SX, Jung D, Yao R. ShinyGO: a graphical gene-set enrichment tool for animals and plants. Bioinformatics. 2020 Apr 15;36(8):2628-9.

141. Letunic I, Bork P. Interactive Tree of Life (iTOL) v6: recent updates to the phylogenetic tree display and annotation tool. Nucleic Acids Research. 2024 Apr 13:gkae268.

1169 # Supporting information captions

1170 **S1. Figure. Differenced of growth patterns of the *P. aeruginosa* AMT 0023-30 early infection isolate**
1171 **with different inoculation volumes.**

1172 **S2. Figure. Differences in doubling times of the *P. aeruginosa* AMT 002330 early infection strain in**
1173 **hypoxic and normoxic conditions. A.** OD_{600} measurements over time. **B.** CFU/ml counts over time **C.**
1174 OD_{600} to CFU/ml trend lines and linear regression calculations. **D.** Differences in generation times in
1175 normoxia and hypoxia.

1176 **S3. Table. Proteins differentially expressed after 28 day exposure to hypoxia**

1177 **S4. Table. Functional enrichment of proteins changed in abundance after 28 days of exposure to**
1178 **hypoxia**

1179

1180

1181

1182

1183

1184

1185

1186

1187

1188

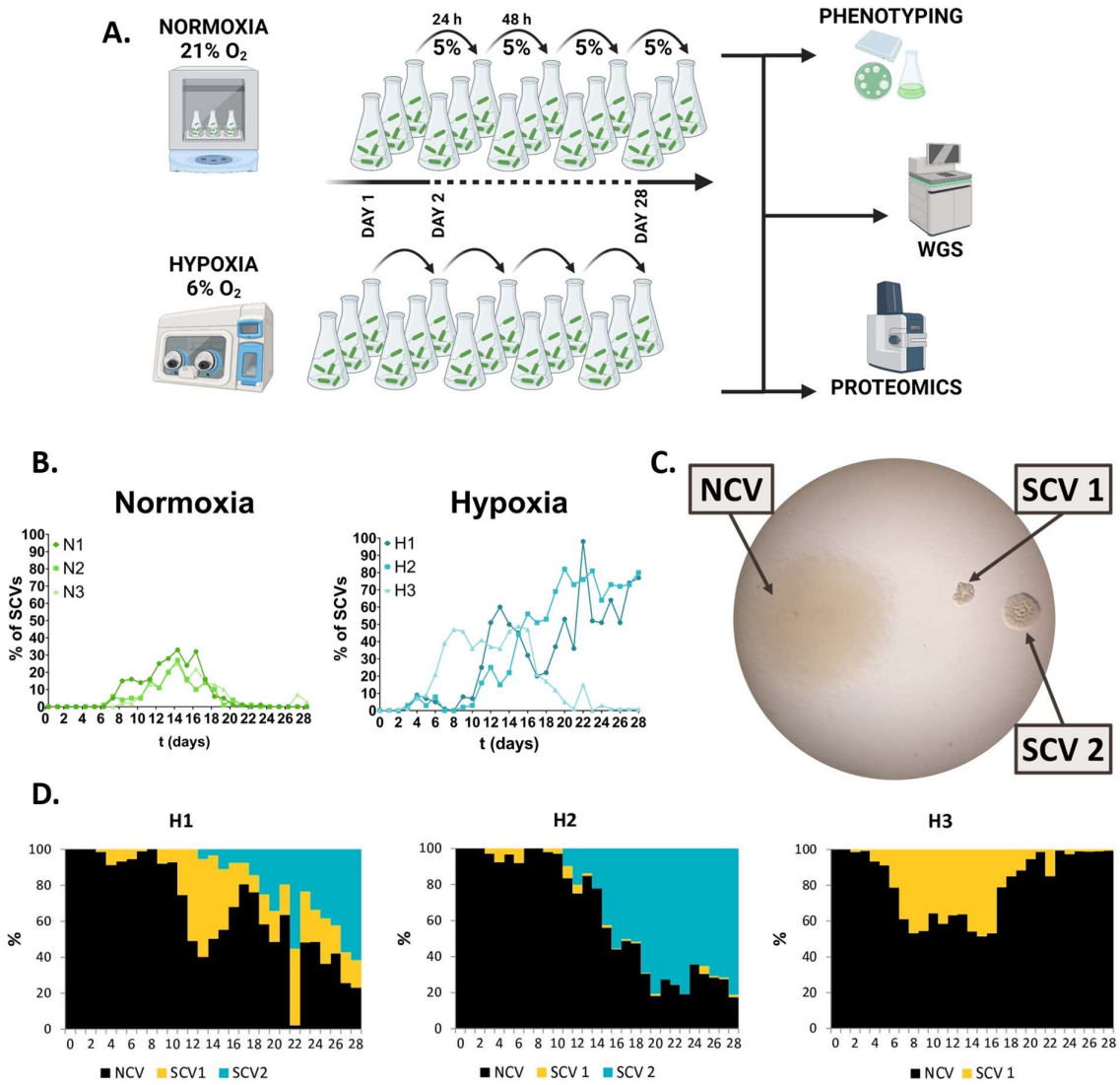

Figure 1. Long-term adaptation of *Pseudomonas aeruginosa* to hypoxic conditions. Experimental evolution study design (**A.**) and influence of hypoxia on small colony variants emergence **B.** Percentage of SCVs in individual normoxia- and hypoxia adapting cultures over 28 days. **C.** Hypoxia-adapted colony morphotypes observed throughout the long-term adaptation. **D.** Ratios of SCV 1 and SCV 2 in the hypoxia-adapting populations over 28 days. The percentage of the small colony variants in the whole populations was caried out for each flask individually each day of the experiment.

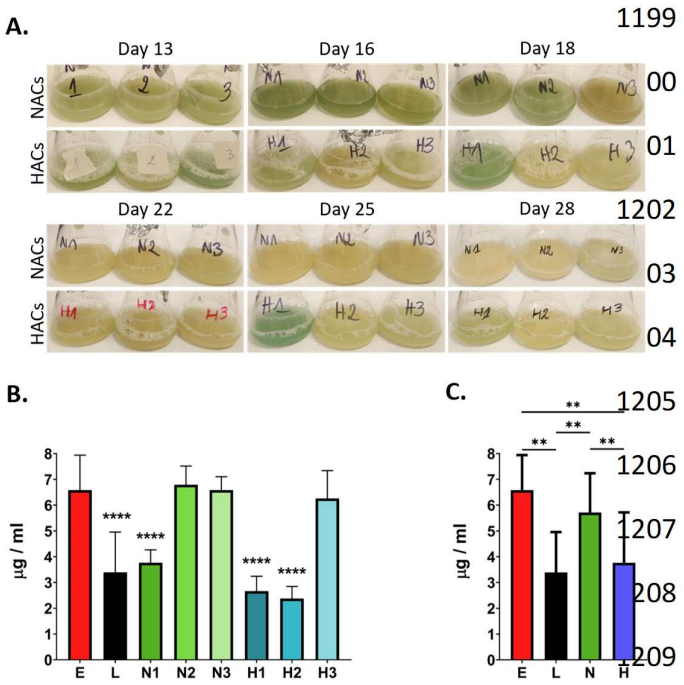

Figure 2. Influence of hypoxia on pyocyanin production. A. Representative photographs of flasks during the 28 day experimental evolution study showing changes in pyocyanin production. **B.** Quantification of pyocyanin production by individual populations. **C.** Quantification of pyocyanin production, pooled data for normoxia- and hypoxia-adapted cultures. The data represents the concentration of pyocyanin in 1ml of bacterial culture, calculated as described in the methods. The data represents two separate experiments performed in normoxic conditions, with at least 3 technical replicates for each strain. Statistically significant differences by ordinary one-way ANOVA test compared to the early infection strain with an uncorrected Fishers LSD test (B.) or Kruskal-Wallis one-way ANOVA test comparing all groups with an uncorrected Dunn's test (C.) are shown (**p< 0.01; ***p<0.001; ****p< 0.0001). E: early infection clinical isolate; L: late infection clinical isolate; N1, N2, N3: 28-day normoxia-adapted populations; H1, H2, H3: 28-day hypoxia adapted populations.

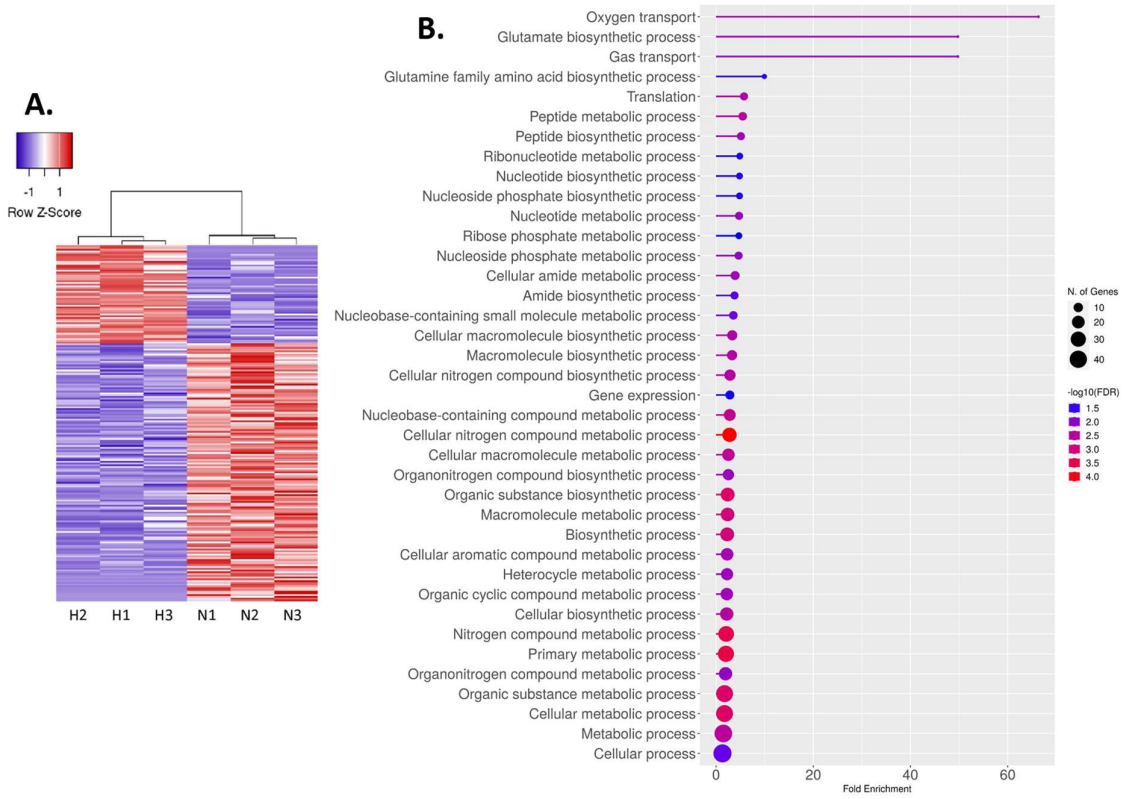

Figure 3. Whole proteome comparison of long-term hypoxia-adapted and normoxia-adapted *P. aeruginosa.* **A.** Heat map representing expression patterns in adapted populations. The heatmap was generated with the use of Heatmapper (Babicki et al., 2016). **B.** Dot plot representing functional GoTerm Biological Process enrichment of proteins with increased and decreased abundance in hypoxia. The enrichment analysis and dot plot were prepared using ShinyGo 0.80 (140).

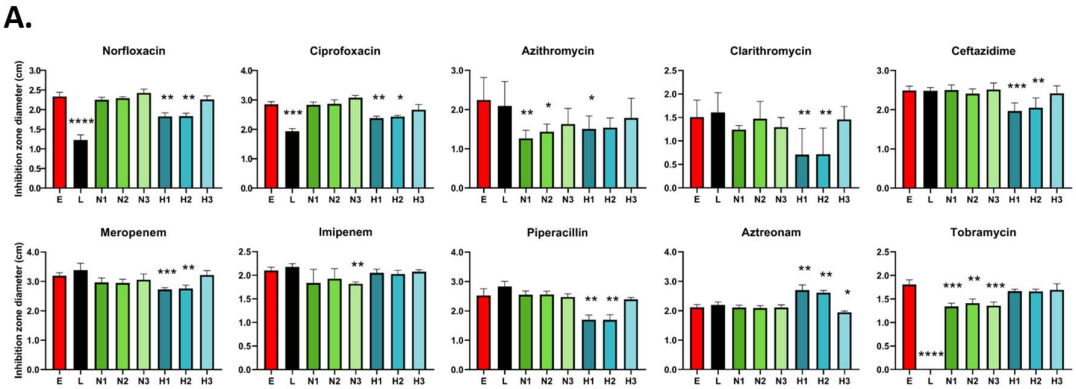

B.

Antibiotic	L	N1	N2	N3	H1	H2	H3	Antibiotic Class
Norfloxacin	↑	=	=	=	↑	↑	=	Fluoroquinolones
Ciprofoxacin	↑	=	=	=	↑	↑	=	
Azithromycin	=	↑	↑	=	↑	=	=	Macrolides
Clarithromycin	=	=	=	=	↑	↑	=	
Ceftazidime	=	=	=	=	↑	↑	=	Cephalosporins
Cefotaxime	=	=	=	=	=	=	=	
Meropenem	=	=	=	=	↑	↑	=	Carbapenems
Imipenem	=	=	=	↑	=	=	=	
Tobramycin	↑R	↑	↑	↑	=	=	=	Aminoglycosides
Piperacillin	↓	=	=	=	↑	↑	=	Penicillins
Aztreonam	=	=	=	=	↓	↓	↑	Monobactams
Tetracycline	= R	= R	= R	= R	= R	= R	= R	Tetracyclines

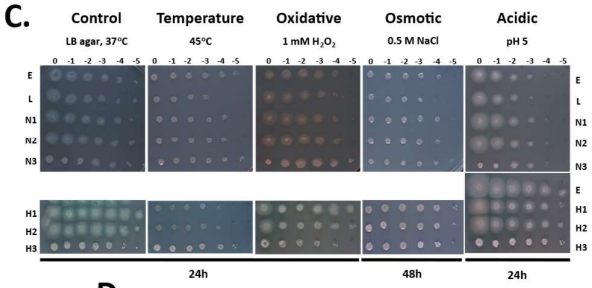

D.

Stress type	L	N1	N2	N3	H1	H2	H3
Temperature	↓	↓	↓	=	↓	↓	=
Osmotic	↓	↑	=	↑	↑	↑	↑
Oxidative	=	=	=	↑	↑	↑	=
Acidic	=	↑	↑	↑	=	=	=

Figure 4. Effects of long-term hypoxia adaptation on antibiotic resistance and stress resistance. **A.** Graphs represent the antibiotic susceptibility of early infection control strain AMT 0023-30, late infection strain, AMT 0023-31, and 28-day adapted populations using diffusion discs, tested in normoxic conditions. Bars represent the mean inhibition zone diameter. The data represents three biological replicates and error bars represent the standard deviation. The significance was determined with the nonparametric Kruskal-Wallis test in combination with uncorrected Dunns multiple comparisons test. **B**. Summary of resistance to all tested antibiotics. **C.** Droplet assays. Representative pictures of colonies from serial dilutions of each strain plated on agar with stress factor added, tested in normoxic conditions. The experiment was performed at least 3 times for each stress type with the early infection isolate as a control. **D.** Table summarising changes in stress sensitivity. ↑ - increased resistance; ↓ - decreased resistance; = no significant difference in resistance; R – no inhibition zone observed. E: early infection clinical isolate; L: late infection clinical isolate; N1, N2, N3: 28-day normoxia-adapted populations; H1, H2, H3: 28-day hypoxia adapted populations.

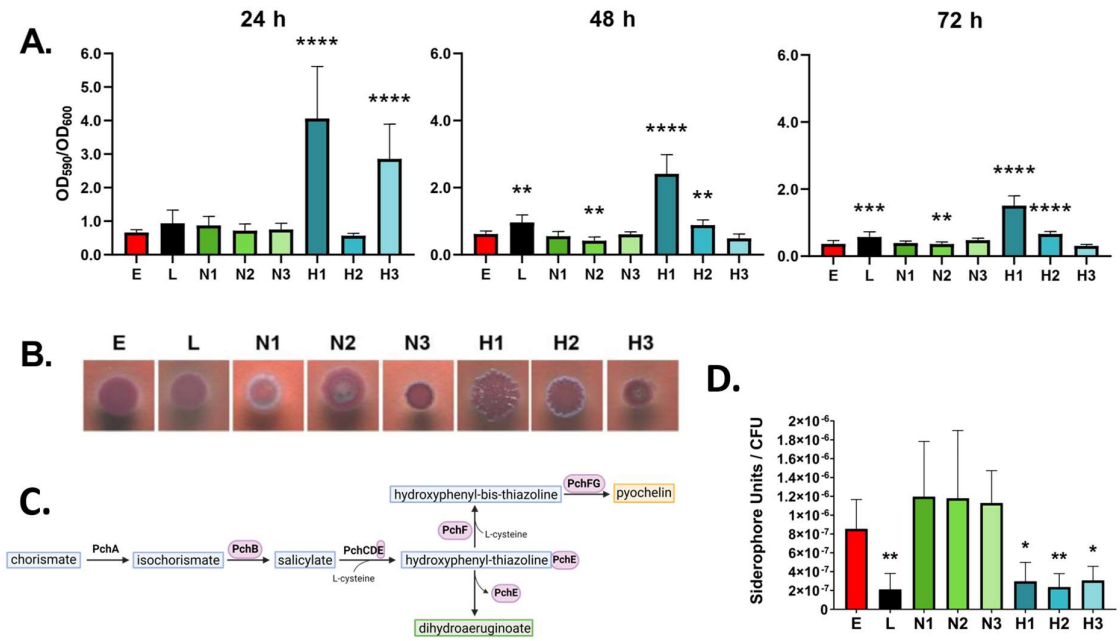

Figure 5. Effects of long-term hypoxia adaptation on biofilm formation, exopolysaccharide production and siderophore production. A. Biofilm formation capability of hypoxia-adapted cultures determined with the crystal violet assay after 24, 48 or 72h of static incubation on a 96-well plate in normoxic conditions. Data represents the mean value of the OD_{590}/OD_{600} ratio from three separate experiments with at least 6 technical replicates for each strain. Statistically significant difference by Kruskal-Wallis one-way ANOVA test compared to the early infection strain (E) with an uncorrected Dunn's test (**p< 0.01; ***p<0.001; ****p< 0.0001). **B.** Exopolysaccharide production by the adapted cultures. The photographs show colonies of different populations of bacteria. The change of colour to a darker shade and a wrinkly colony surface indicate a higher exopolysaccharide production. **C.** Pathway of pyochelin synthesis. Pink: proteins decreased in abundance in the proteome of hypoxia-adapted populations. **D.** Siderophore production represented as an average of siderophore units produced by each colony forming unit, tested in normoxic conditions. Statistically significant differences by ordinary one-way ANOVA test compared to the early infection strain with an uncorrected Fishers LSD test are shown (*p<0.05; **p< 0.01). E: early infection clinical isolate; L: late infection clinical isolate; N1, N2, N3: 28-day normoxia-adapted populations; H1, H2, H3: 28-day hypoxia adapted populations. E: early infection clinical isolate, AMT 0023-30; L: late infection clinical isolate, AMT 0023-31; N1, N2, N3: 28-day normoxia-adapted populations; H1, H2, H3: 28-day hypoxia adapted populations.

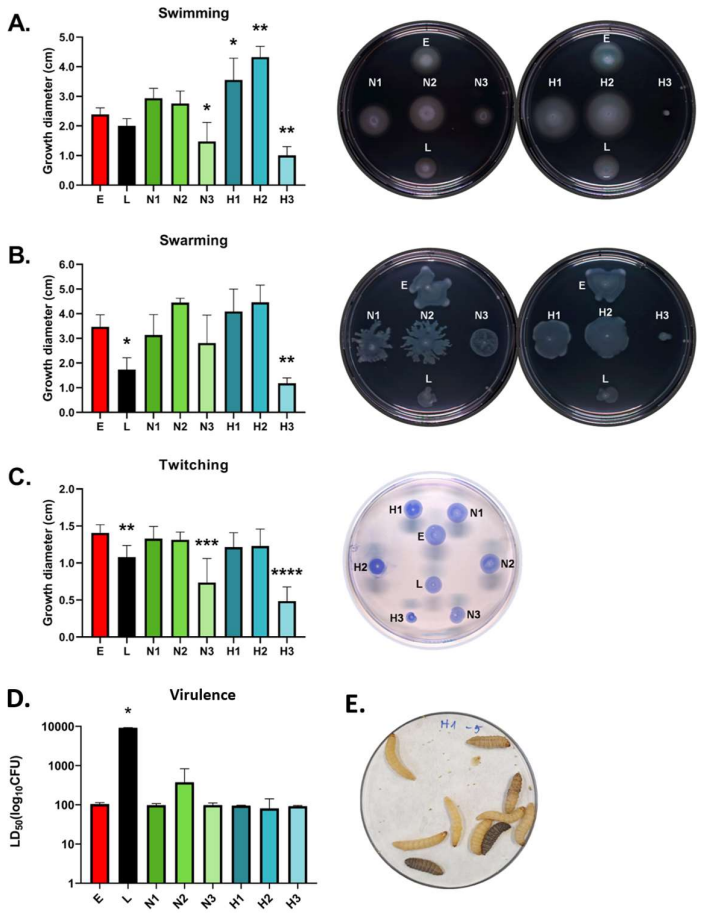

Figure 6. Effects of long-term hypoxia adaptation on *P. aeruginosa* motility and virulence in the *Galleria mellonela* model. A. Changes in swimming motility**. B.** Changes in swarming motility. **C.** Changes in twitching motility. For each type of motility, a graph representing the average of diameter of the colony with bars representing data from at least 3 separate experiments conducted in normoxic conditions, with at least two technical replicates. Statistically significant difference by Kruskal-Wallis one-way ANOVA test compared to the early infection strain (E) with an uncorrected Dunn's test (*p< 0.05; **p< 0.01; ***p<0.001; ****p< 0.0001). **D.** Graph representing the average CFU needed to reach LD50 within 24h of the experiment from at least 3 separate repeats of the experiment**.** A touch to the larvae head was used to determine if they are alive. Statistically significant difference by Kruskal-Wallis one-way ANOVA test compared to the early infection strain (E) with an uncorrected Dunn's test is presented (*p< 0.05). **E.** A representative picture showing the *G. mellonela* larvae melanisation. Healthy larvae with no disease symptoms are a bright cream colour. Larvae showing a slightly beige colour show first symptoms of infection, larvae with dark spots/stipes are clearly affected and the severely melanised larvae are in the late stages of the infection or dead. E: early infection clinical isolate; L: late infection clinical isolate; N1, N2, N3: 28-day normoxia-adapted populations; H1, H2, H3: 28 day hypoxia adapted populations.

A.

Phenotype		L	N1	N2	N3	H1	H2	H3
SCVs (%)		58.0%	0.00	0.00	2.7%	76.9%	79.8%	0.7%
Pyocyanin		↓	↓	=	=	↓	↓	=
Antibiotic resistance		=	=	=	=	↑	↑	=
Stress resistance	Osmotic	↓	↑	=	↑	↑	↑	↑
	Oxidative	=	=	=	↑	↑	↑	=
	Heat	↓	↓	↓	=	↓	↓	=
	Acidic	=	↑	↑	↑	=	=	=
Biofilm 72h		↑	=	↑	=	↑	↑	=
Motility	Swimming	↓	↑	↑	↓	↑	↑	↓
	Swarming	↓	=	↑	↓	↑	↑	↓
	Twitching	↓	=	↑	=	=	↑	↓
Siderophore production		↓	=	=	=	↓	↓	↓
Virulence (*Galleria mellonela*)		↑	=	=	=	=	=	=

B.

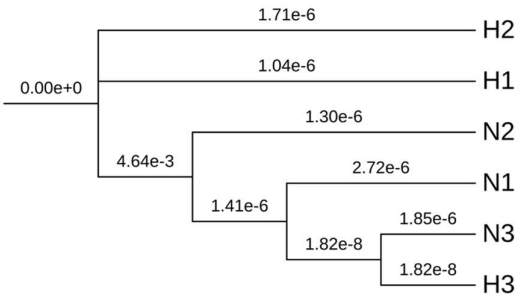

Figure 7. Patterns of adaptation to long-term hypoxia. A. Summary of the phenotypic changes of adapted cultures tested in normoxic conditions. **B.** Phylogenetic tree of adapted *P. aeruginosa* populations generated by the iTOL Interactive tree of life (v6) (141). The branch lengths are presented for each isolate.